Relations between generalized parton distributions and transverse momentum dependent parton distributions

Bheemsehan Gurjar,[1] Dipankar Chakrabarti,[1] Poonam Choudhary,[1] Asmita Mukherjee,[2] and Pulak Talukdar[1]
[1]*Indian Institute of Technology, Kanpur, Kanpur-208016, India*
[2]*Indian Institute of Technology, Bombay, Powai, Mumbai 400076, India*

(Received 13 July 2021; accepted 29 September 2021; published 27 October 2021)

We investigate the relations between transverse momentum dependent parton distributions (TMDs) and generalized parton distributions (GPDs) in a light-front quark-diquark model motivated by soft-wall AdS/QCD. Many relations are found to have similar structure in different models. It is found that a relation between the Sivers function and the GPD E_q can be obtained in this model in terms of a lensing function. The quark orbital angular momentum is calculated and the results are compared with the results in other similar models. Implications of the results are discussed. Relations among different TMDs in the model are also presented.

DOI: 10.1103/PhysRevD.104.076028

I. INTRODUCTION

Understanding the structure of the nucleon in terms of its fundamental constituents, quarks and gluons, in three dimensions has attracted quite a lot of interest in hadron physics in recent days. These are investigated in terms of the different distributions of quarks and gluons that encode their internal dynamics, as well as the correlations between the intrinsic momentum and spin. The parton distributions are probed traditionally in high energy scattering experiments, where the interactions take place through the quarks and gluons, and the scattering cross section depends on the probability to find a quark with momentum fraction x inside the parent nucleon at a given momentum scale (energy of the experiment). These are called collinear parton distributions as they are not sensitive to the intrinsic transverse momentum of the quarks and gluons. However, single spin asymmetries observed in semi-inclusive deep inelastic scattering (SIDIS) or Drell-Yan (DY) processes, where the target or one of the proton beams is polarized, depend on transverse momentum dependent parton distribution (TMDs) [1] that give the distribution of quarks and gluons in three-dimensional momentum space. The TMDs are functions of the longitudinal momentum fraction x and transverse momentum p_T of the partons. There are eight leading quark TMDs for the proton, each encode a different momentum-momentum or momentum-spin correlation. These TMDs can be expressed in terms of the quark field operators, and in order to have color gauge invariance one needs the inclusion of a Wilson line or gauge link. Also known as the initial and/or final state interaction, these basically resum the soft gluon exchanges between the hard part and the soft part of the process. The gauge links are process dependent and thus they introduce a process dependence in the TMDs. For the so-called time reversal odd (T-odd) TMDs like Sivers function or Boer-Mulders function the inclusion of the gauge link is essential [2].

Another set of observables that have gained a lot of interest in recent days are the generalized parton distributions (GPDs) of the nucleon [3]. These are probed in exclusive processes like the deeply virtual Compton scattering or the deeply virtual meson production. GPDs can be expressed in terms of off-forward matrix elements of a bilocal operator, and these do not have probabilistic interpretation. There are eight leading GPDs for the quarks. In the forward limit or when the momentum transfer in the process is zero, GPDs reduce to the collinear parton distribution function (pdf); whereas when integrating them over x one gets the form factors. When the momentum transfer Δ_T is purely in the transverse direction, by taking a Fourier transform with respect to Δ_T one obtains impact parameter dependent parton distributions (IPDpdfs) [4] that are functions of x and the transverse impact parameter b_T. These have a probabilistic interpretation: they give the distribution of quarks with longitudinal momentum fraction x in the b_T plane.

As a matter of fact, there is no direct one-to-one correspondence between the TMDs and GPDs. This is because b_T and p_T are not Fourier conjugate variable to each other. b_T is the Fourier conjugate to the momentum transfer Δ_T, and p_T may be interpreted as the average momentum of the active quark. However, b_T and p_T obey

Heisenberg's uncertainty principle as the corresponding operators do not commute. So although both the GPDs and TMDs give a three-dimensional quark-gluon picture of the nucleon, one is not related to the other through a Fourier transform. A model-independent connection between the GPDs and the TMDs can be obtained through the generalized transverse momentum dependent pdfs (GTMDs) or Wigner functions, which are Fourier transforms of the GTMDs [5,6]. These give the most general tomographic picture of the nucleon. Integration over b_T sets $\Delta_T = 0$ and the Wigner distributions become the TMD correlators. On the other hand, integrating over p_T sets transverse separation $z_T = 0$ and they reduce to IPDpdfs.

However, in some models, certain relations between the TMDs and GPDs are found to hold. One such relation is between the Sivers function and the GPD E_q in impact parameter space, in some particular model where the final state interaction can be factored out in what is called a "chromodynamic lensing function" [7,8]. This gives an intuitive picture of the Sivers effect in such models in terms of distortions in transverse impact parameter space, due to the nonzero orbital angular momentum of the active quark. Such relations do not hold if higher-order corrections are included. Thus, model-dependent relations are important as they help to understand the physics related to these TMDs in the framework of the effective theory on which such models are based. In [9], a systematic study of all possible nontrivial model-dependent relations between TMDs and GPDs was performed and such relations were arranged in four categories depending on the number of derivatives in impact parameter space. In [10] it was shown that the relation connecting a T-odd TMD to a distortion in impact parameter space through a lensing function holds only in models where the nucleon is described as a two-particle bound state, like a quark and a diquark. Further, such relations are not satisfied if axial-vector diquarks are included in the model.

In the present work, we investigate model relations in a light-front diquark model where the analytic form of the light-front wave functions (LFWF) is motivated by the AdS/QCD correspondence. The model includes both scalar and axial-vector diquarks [11]. Total nucleon wave functions are obtained by the light-front holographic wave function multiplied by the momentum dependent helicity wave functions. Finally, we incorporate the final state interaction in the wave functions to evaluate the T-odd TMDs. We also calculate the orbital angular momentum of the quarks in this model and discuss the results.

The plan of the paper is as follows. In Sec. II, we introduce the light-front quark-diquark model used in this work. The modification of the wave functions to incorporate the final state interaction (FSI) effect is given in Sec. II A. Then, in Sec. III, we define the GPDs and TMDs in this model. Model-independent relations among the GPDs and TMDs are also presented in this section. Then we present the model-dependent relations between the GPDs and TMDs in Sec. IV. The model result of the lensing function is discussed in Sec. IV B and the relations among different TMDs are presented in Sec. V. In Sec. VI, different definitions of orbital angular momentum in terms of GPDs and TMDs are evaluated. Finally, we conclude the paper in Sec. VII.

II. LIGHT-FRONT QUARK-DIQUARK MODEL

Here we briefly introduce the light-front quark-diquark model developed in [11,12] with the wave functions modeled from the effective two-particle wave function predicted by AdS/QCD. The particular model of nucleons employed in this work is considered to be a linear combination of a quark-diquark state including both the scalar diquark and axial-vector diquarks [11]. With the $SU(4)$ spin-flavor structure, the proton states can be written as [13]

$$|P;\pm\rangle = C_{\mathrm{S}}|uS^0\rangle^{\pm} + C_{\mathrm{V}}|uA^0\rangle^{\pm} + C_{\mathrm{VV}}|dA^1\rangle^{\pm}. \quad (1)$$

S and A represent the scalar and axial-vector diquarks with isospin at their superscripts. Under the isospin symmetry, the neutron state can be obtained from the above expression [Eq. (1)] with the interchange of $u \leftrightarrow d$. The two-particle Fock state expansion for $J^z = \pm\frac{1}{2}$ for a spin-0 diquark is given by

$$\begin{aligned}|uS\rangle^{\pm} = \int \frac{\mathrm{d}x\mathrm{d}^2\mathbf{p}_T}{2(2\pi)^3\sqrt{x(1-x)}} \\ \times \left[\psi_{+}^{\pm(u)}(x,\mathbf{p}_T)\left|+\frac{1}{2},0;xP^+,\mathbf{p}_T\right\rangle\right. \\ \left. + \psi_{-}^{\pm(u)}(x,\mathbf{p}_T)\left|-\frac{1}{2},0;xP^+,\mathbf{p}_T\right\rangle\right], \end{aligned} \quad (2)$$

where $|\lambda_q, 0; xP^+, \mathbf{k}_T\rangle$ represents the two-particle Fock state with an active quark with helicity $\lambda_q = \pm\frac{1}{2}$ and carrying longitudinal momentum xP^+ and transverse momentum $\mathbf{k}_T$, and a scalar diquark with helicity $\lambda_S = 0$. Similarly the state with a spin-1 diquark is given as

$$\begin{aligned}|vA\rangle^{\pm} = \int \frac{\mathrm{d}x\mathrm{d}^2\mathbf{p}_T}{2(2\pi)^3\sqrt{x(1-x)}} \\ \times \left[\psi_{++}^{\pm(v)}(x,\mathbf{p}_T)\left|+\frac{1}{2}+1;xP^+,\mathbf{p}_T\right\rangle\right. \\ + \psi_{-+}^{\pm(v)}(x,\mathbf{p}_T)\left|-\frac{1}{2}+1;xP^+,\mathbf{p}_T\right\rangle + \psi_{+0}^{\pm(v)}(x,\mathbf{p}_T)\left|\right. \\ \left. +\frac{1}{2}0;xP^+,\mathbf{p}_T\right\rangle + \psi_{-0}^{\pm(v)}(x,\mathbf{p}_T)\left|-\frac{1}{2}0;xP^+,\mathbf{p}_T\right\rangle \\ + \psi_{+-}^{\pm(v)}(x,\mathbf{p}_T)\left|+\frac{1}{2}-1;xP^+,\mathbf{p}_T\right\rangle \\ \left. + \psi_{--}^{\pm(v)}(x,\mathbf{p}_T)\left|-\frac{1}{2}-1;xP^+,\mathbf{p}_T\right\rangle\right], \end{aligned} \quad (3)$$

where $|\lambda_q, \lambda_A; xP^+, \mathbf{p}_T\rangle$ represents a two-particle state with a quark of helicity $\lambda_q = \pm\frac{1}{2}$ and an axial-vector diquark with helicity $\lambda_A = \pm 1, 0$(triplet).

A. Final state interaction and T-odd TMDs

The FSIs [14] provide a nontrivial phase in the amplitude which is required to produce nonvanishing spin asymmetries in SIDIS processes associated with T-odd TMDs. In this model, the contribution of the FSI is included in the light-front wave functions [15] to evaluate the leading twist T-odd TMDs, i.e., the Sivers function, $f_{1T}^{\perp q}(x, \mathbf{p}_T^2)$, and the Boer-Mulders function, $h_1^{\perp q}(x, \mathbf{p}_T^2)$. With the inclusion of FSI, the process dependent wave functions [16] are given by (a) for scalar diquark,

$$\begin{aligned}
\psi_{+}^{(u)}(x,\mathbf{p}_T) &= N_S\left[1 + i\frac{e_1e_2}{8\pi}(\mathbf{p}_T^2 + B)g_1\right]\varphi_1^{(u)}(x,\mathbf{p}_T)\\
\psi_{-}^{+(u)}(x,\mathbf{p}_T) &= N_S\left(-\frac{p^1 + ip^2}{xM}\right)\left[1 + i\frac{e_1e_2}{8\pi}(\mathbf{p}_T^2 + B)g_2\right]\varphi_2^{(u)}(x,\mathbf{p}_T)\\
\psi_{+}^{-(u)}(x,\mathbf{p}_T) &= N_S\left(\frac{p^1 - ip^2}{xM}\right)\left[1 + i\frac{e_1e_2}{8\pi}(\mathbf{p}_T^2 + B)g_2\right]\varphi_2^{(u)}(x,\mathbf{p}_T)\\
\psi_{-}^{(u)}(x,\mathbf{p}_T) &= N_S\left[1 + i\frac{e_1e_2}{8\pi}(\mathbf{p}_T^2 + B)g_1\right]\varphi_1^{(u)}(x,\mathbf{p}_T),
\end{aligned} \tag{4}$$

(b) for axial-vector diquark (for $J = +1/2$),

$$\begin{aligned}
\psi_{++}^{+(\nu)}(x,\mathbf{p}_T) &= N_1^{(\nu)}\sqrt{\frac{2}{3}}\left(\frac{p^1 - ip^2}{xM}\right)\left[1 + i\frac{e_1e_2}{8\pi}(\mathbf{p}_T^2 + B)g_2\right]\varphi_2^{(\nu)}(x,\mathbf{p}_T)\\
\psi_{-+}^{+(\nu)}(x,\mathbf{p}_T) &= N_1^{(\nu)}\sqrt{\frac{2}{3}}\left[1 + i\frac{e_1e_2}{8\pi}(\mathbf{p}_T^2 + B)g_1\right]\varphi_1^{(\nu)}(x,\mathbf{p}_T)\\
\psi_{+0}^{+(\nu)}(x,\mathbf{p}_T) &= -N_0^{(\nu)}\sqrt{\frac{1}{3}}\left[1 + i\frac{e_1e_2}{8\pi}(\mathbf{p}_T^2 + B)g_1\right]\varphi_1^{(\nu)}(x,\mathbf{p}_T)\\
\psi_{-0}^{+(\nu)}(x,\mathbf{p}_T) &= N_0^{(\nu)}\sqrt{\frac{1}{3}}\left(\frac{p^1 + ip^2}{xM}\right)\left[1 + i\frac{e_1e_2}{8\pi}(\mathbf{p}_T^2 + B)g_2\right]\varphi_2^{(\nu)}(x,\mathbf{p}_T)\\
\psi_{+-}^{+(\nu)}(x,\mathbf{p}_T) &= 0\\
\psi_{--}^{+(\nu)}(x,\mathbf{p}_T) &= 0,
\end{aligned} \tag{5}$$

and, for $J = -1/2$,

$$\begin{aligned}
\psi_{++}^{-(\nu)}(x,\mathbf{p}_T) &= 0\\
\psi_{-+}^{-(\nu)}(x,\mathbf{p}_T) &= 0\\
\psi_{+0}^{-(\nu)}(x,\mathbf{p}_T) &= N_0^{(\nu)}\sqrt{\frac{1}{3}}\left(\frac{p^1 - ip^2}{xM}\right)\left[1 + i\frac{e_1e_2}{8\pi}(\mathbf{p}_T^2 + B)g_2\right]\varphi_2^{(\nu)}(x,\mathbf{p}_T)\\
\psi_{-0}^{-(\nu)}(x,\mathbf{p}_T) &= N_0^{(\nu)}\sqrt{\frac{1}{3}}\left[1 + i\frac{e_1e_2}{8\pi}(\mathbf{p}_T^2 + B)g_1\right]\varphi_1^{(\nu)}(x,\mathbf{p}_T)\\
\psi_{+-}^{-(\nu)}(x,\mathbf{p}_T) &= -N_1^{(\nu)}\sqrt{\frac{2}{3}}\left[1 + i\frac{e_1e_2}{8\pi}(\mathbf{p}_T^2 + B)g_1\right]\varphi_1^{(\nu)}(x,\mathbf{p}_T)\\
\psi_{--}^{-(\nu)}(x,\mathbf{p}_T) &= N_1^{(\nu)}\sqrt{\frac{2}{3}}\left(\frac{p^1 + ip^2}{xM}\right)\left[1 + i\frac{e_1e_2}{8\pi}(\mathbf{p}_T^2 + B)g_2\right]\varphi_2^{(\nu)}(x,\mathbf{p}_T),
\end{aligned} \tag{6}$$

TABLE I. In the light-front AdS/QCD axial-vector diquark model, the values of the fitted parameters for u and d quarks at $\mu_0 = 0.313$ GeV.

ν	a_1^ν	b_1^ν	a_2^ν	b_2^ν	δ^ν
u	0.280 ± 0.001	0.1716 ± 0.0051	0.84 ± 0.02	0.2284 ± 0.0035	1.0
d	0.5850 ± 0.0003	0.7000 ± 0.0002	$0.9434^{+0.0017}_{-0.0013}$	$0.64^{+0.0082}_{-0.0022}$	1.0

where,

$$g_1 = \int_0^1 d\alpha \frac{-1}{\alpha(1-\alpha)\mathbf{p}_T^2 + \alpha m_g^2 + (1-\alpha)B}, \quad (7)$$

$$g_2 = \int_0^1 d\alpha \frac{-\alpha}{\alpha(1-\alpha)\mathbf{p}_T^2 + \alpha m_g^2 + (1-\alpha)B}, \quad (8)$$

and

$$B = x(1-x)\left(-M^2 + \frac{m_q^2}{x} + \frac{m_D^2}{1-x}\right). \quad (9)$$

Here, M, m_q, m_D and m_g are the masses of the proton, struck quark, diquark, and the gluon, respectively. e_1 and e_2 are the color charges of the struck quark and diquark, and the FSI gauge exchange strength is $\frac{e_1 e_2}{4\pi}$. We take $m_g = 0$ at the end of the calculations. N_s, N_0^ν, and N_1^ν are the normalization constants. The LFWFs $\varphi_i^\nu(x, \mathbf{p}_T)$ are modified from the soft-wall AdS/QCD predictions as [11]

$$\varphi_i^{(\nu)}(x, \mathbf{p}_T) = A_i^\nu(x) \exp[-a(x)\mathbf{p}_T^2], \quad (10)$$

with

$$A_i^\nu(x) = \frac{4\pi}{\kappa}\sqrt{\frac{\log(\frac{1}{x})}{1-x}} x^{a_i^\nu}(1-x)^{b_i^\nu}, \quad (11)$$

and

$$a(x) = \delta^\nu \frac{\log(\frac{1}{x})}{\kappa^2(1-x)^2}. \quad (12)$$

The parameters a_i^ν, b_i^ν, and δ^ν are obtained by fitting the electromagnetic form factors. The wave function [Eq. (10)] reduces to the AdS/QCD prediction [17] for the parameters $a_i^\nu = b_i^\nu = 0$ and $\delta^\nu = 1$. We use the AdS/QCD scale parameter $\kappa = 0.4$ GeV [18] and the quark masses are assumed to be zero. For completeness and to be self-contained, we list the parameters obtained in Ref. [11]. The normalization constants are $N_s = 2.0191$, $N_0^u = 3.2050$, $N_0^d = 5.9423$, $N_1^u = 0.9895$, $N_1^d = 1.1616$, $C_s^2 = 1.3872$, $C_V^2 = 0.6128$, and $C_{VV}^2 = 1.0$, and the other parameters are listed in Table I. Henceforth, we refer to this model as the LFQDQ model.

The nucleon parton distributions like GPDs, TMDs, and Wigner distributions are already calculated in this model and the model has been shown to reproduce different spin asymmetries in the SIDIS processes [16,19–22]. TMDs, Wigner distributions, and Husimi distributions are also calculated in a light-front quark-diquark model in Refs. [23,24]. Recently, gluonic distributions like PDFs, TMDS, GPDs, etc. have also been calculated in AdS/QCD [25,26].

III. DEFINITIONS AND TRIVIAL RELATIONS

A. Generalized parton distributions

The GPDs (for a review, see Ref. [3]) are defined as off-forward matrix elements of the bilocal operator of light-front correlation functions of vector, axial-vector, and tensor current. The off-forward correlator is given by

$$F^{q[\Gamma]}(x, \Delta; \lambda, \lambda') = \frac{1}{2}\int \frac{dz^-}{2\pi} e^{ik\cdot z}\left\langle P'; \lambda'|\bar{\psi}\left(-\frac{1}{2}z\right)\Gamma \times \mathcal{W}_{\mathrm{GPD}}\left(-\frac{1}{2}z; \frac{1}{2}z\right)\psi\left(\frac{1}{2}z\right)|P; \lambda\right\rangle\Big|_{z^+=0^+, \mathbf{z}_T=\mathbf{0}_T}, \quad (13)$$

where $P(P')$ and $\lambda(\lambda')$ denote the momenta and the helicity of the initial (final) state of the proton, respectively. The object Γ is a generic matrix in Dirac space, at leading twist; it can be $\gamma^+, \gamma^+\gamma^5$, or $\sigma^{+\perp}\gamma^5$. The Wilson line, $\mathcal{W}_{\mathrm{GPD}}$, is required for gauge invariance of the correlator and is given by

$$\mathcal{W}_{\mathrm{GPD}}\left(-\frac{1}{2}z; \frac{1}{2}z\right)\Big|_{z^+=0^+, \mathbf{z}_T=\mathbf{0}_T} = \left[0^+, -\frac{1}{2}z^-, \mathbf{0}_T; 0^+, \frac{1}{2}z^-, \mathbf{0}_T\right] = \mathcal{P}\exp\left(-ig\int_{-(1/2)z^-}^{(1/2)z^-} dy^- t_a A_a^+(0^+, y^-, \mathbf{0}_T)\right), \quad (14)$$

where $\mathcal{P}$ is the path ordering and t_a represents the Gell-Mann matrices. For the three particular Γ in Eq. (13) we can obtain the leading twist GPDs [9] as

$$F^{q[\gamma^+]}(x,\Delta;\lambda,\lambda') = \frac{1}{2\bar{P}^+}\bar{u}(P',\lambda')\left[H^q\gamma^+ + E^q\frac{i}{2M}\sigma^{+\alpha}\Delta_\alpha\right]u(P,\lambda), \tag{15}$$

$$F^{q[\gamma^+\gamma_5]}(x,\Delta;\lambda,\lambda') = \frac{1}{2\bar{P}^+}\bar{u}(P',\lambda')\left[\tilde{H}^q\gamma^+\gamma_5 + \tilde{E}^q\frac{\gamma_5\Delta^+}{2M}\right]u(P,\lambda), \tag{16}$$

$$F^{q[\sigma^{+j}\gamma_5]}(x,\Delta;\lambda,\lambda') = \frac{1}{2\bar{P}^+}\bar{u}(P',\lambda')\left[H_T^q\sigma^{+j}\gamma_5 + \tilde{H}_T^q\frac{\epsilon^{+j\alpha\beta}\Delta_\alpha P_\beta}{M^2} + E_T^q\frac{\epsilon^{+j\alpha\beta}\Delta_\alpha\gamma_\beta}{2M} + \tilde{E}_T^q\frac{\epsilon^{+j\alpha\beta}P_\alpha\gamma_\beta}{M}\right]u(P,\lambda), \tag{17}$$

where M denotes the mass of the proton and $j = 1, 2$ is a transverse index, $\bar{P} = (P + P')/2$ denotes the average nucleon momentum, and $\Delta = P' - P$ is the momentum transfer to the nucleon. The H and E, the so-called unpolarized GPDs, and the helicity dependent GPDs, $\tilde{H}$ and $\tilde{E}$ are chiral-even, while H_T, $\tilde{H}_T$, E_T, and $\tilde{E}_T$ are chiral-odd. There exist eight leading twist quark GPDs. All GPDs are real valued which follows from time-reversal and depend on the three variables $x = \frac{p^+}{\bar{P}^+}$, $\xi = -\frac{\Delta^+}{2\bar{P}^+}$, and $t = -Q^2 = \Delta^2$; where the light-cone coordinates are defined as $x^\pm = \frac{1}{\sqrt{2}}(x^0 \pm x^3)$, $\mathbf{x}_T = (x^1, x^2)$. We choose the light-front gauge $A^+ = 0$, so that the gauge link appearing in between the quark fields in Eqs. (15)–(17) becomes unity, or, in other words, there is no FSI contribution to the GPDs.

B. GPDs in impact parameter space

The GPDs with zero skewness ($\xi = 0$) in impact parameter space are important for various reasons: (i) the density interpretation of the GPDs holds only in the impact parameter space for zero skewness [27], (ii) the intuitive picture for various transverse single spin asymmetries (SSAs) in semi-inclusive processes is based on the impact parameter representation of GPD E^q [7,28], (iii) it gives an intuitive connection between the Sivers asymmetry and the quark orbital angular momentum in certain models, (iv) the impact parameter representation allows us to make analogies between chiral-odd quark GPDs and TMDs [29]. The parton correlator in impact parameter space is given by the Fourier transform as

$$\mathcal{F}(x,\mathbf{b}_T;S) = \int\frac{d^2\mathbf{\Delta}_T}{(2\pi)^2}\exp(-i\mathbf{\Delta}_T.\mathbf{b}_T)F(x,\mathbf{\Delta}_T;S). \tag{18}$$

Here, S denotes the polarization of the target. The impact parameter $\mathbf{b}_T$ is conjugate to the transverse part of the momentum transfer $\mathbf{\Delta}_T$. The correlator defining the GPDs in impact parameter space is written as

$$\mathcal{F}^{q[\Gamma]}(x,\mathbf{b}_T;S) = \frac{1}{2}\int\frac{dz^-}{2\pi}e^{ixP^+z^-}\langle P^+,\mathbf{0}_T;S|\bar{\psi}(z_1)\Gamma \times \mathcal{W}_{\mathrm{GPD}}(z_1;z_2)\psi(z_2)|P^+,\mathbf{0}_T;S\rangle, \tag{19}$$

with $z_{1/2} = (0^+, \mp\frac{1}{2}z^-, \mathbf{b}_T)$. Although the GPDs are expressed as off-forward matrix elements and do not have a density interpretation, in the impact parameter representation we can obtain diagonal matrix elements and thus impact parameter dependent pdfs have a probabilistic interpretation. The IPDpdfs are given by

$$\mathcal{X}(x,\mathbf{b}_T^2) = \int\frac{d^2\mathbf{\Delta}_T}{(2\pi)^2}e^{-i\mathbf{\Delta}_T\cdot\mathbf{b}_T}X(x,0,-\mathbf{\Delta}_T^2), \tag{20}$$

where $X(x,0,-\mathbf{\Delta}_T^2)$ are the GPDs. The GPD correlators [Eqs. (15)–(17)] for different Γ in the impact parameter space are then obtained [9] as

$$\mathcal{F}^q(x,\mathbf{b}_T;S) = \mathcal{F}^{q[\gamma^+]}(x,\mathbf{b}_T;S) = \mathcal{H}^q(x,\mathbf{b}_T^2) + \frac{\epsilon_T^{ij}b_T^iS_T^j}{M}(\mathcal{E}^q(x,\mathbf{b}_T^2))', \tag{21}$$

$$\tilde{\mathcal{F}}^q(x,\mathbf{b}_T;S) = \tilde{\mathcal{F}}^{q[\gamma^+\gamma_5]}(x,\mathbf{b}_T;S) = \lambda\tilde{\mathcal{H}}^q(x,\mathbf{b}_T^2), \tag{22}$$

$$\begin{aligned}\mathcal{F}_T^{q,j}(x,\mathbf{b}_T;S) &= \mathcal{F}^{q[i\sigma^{j+}\gamma_5]}(x,\mathbf{b}_T;S)\\ &= \frac{\epsilon_T^{ij}b_T^i}{M}(\mathcal{E}_T^q(x,\mathbf{b}_T^2) + 2\tilde{\mathcal{H}}_T^q(x,\mathbf{b}_T^2))'\\ &\quad + S_T^j\left(\mathcal{H}_T^q(x,\mathbf{b}_T^2) - \frac{\mathbf{b}_T^2}{M^2}\Delta_b\tilde{\mathcal{H}}_T^q(x,\mathbf{b}_T^2)\right)\\ &\quad + \frac{2b_T^j\mathbf{b}_T\cdot\mathbf{S}_T - S_T^j\mathbf{b}_T^2}{M^2}(\tilde{\mathcal{H}}_T^q(x,\mathbf{b}_T^2))'',\end{aligned} \tag{23}$$

where

$$(\mathcal{X}(x,\mathbf{b}_T^2))' = \frac{\partial}{\partial\mathbf{b}_T^2}(\mathcal{X}(x,\mathbf{b}_T^2)), \tag{24}$$

$$\Delta_b \mathcal{X}(x, \mathbf{b}_T^2) = \frac{1}{\mathbf{b}_T{}^2} \frac{\partial}{\partial \mathbf{b}_T{}^2} \left[\mathbf{b}_T{}^2 \frac{\partial}{\partial \mathbf{b}_T{}^2} \mathcal{X}(x, \mathbf{b}_T^2) \right]. \quad (25)$$

Equation (21) describes the distribution of unpolarized quarks carrying the longitudinal momentum fraction x at a transverse position b_T. For a transversely polarized target, this distribution has a spin-independent part given by $\mathcal{H}$ and a spin-dependent part proportional to the first order derivative of $\mathcal{E}$. Due to the spin-dependent term, the distribution in impact parameter space is not axially symmetric as it depends on the direction of the impact parameter $\mathbf{b}_T$, i.e., the spin-dependent term causes a distortion of the distribution. This distortion effect can be quantified through the flavor dipole moment [30]:

$$d^{q,i} = \int dx \int d^2\mathbf{b}_T b_T^i \mathcal{F}^q(x, \mathbf{b}_T; S) = -\frac{\epsilon_T^{ij} S_T^j}{2M} \int dx E^q(x, 0, 0) = -\frac{\epsilon_T^{ij} S_T^j}{2M} \kappa^q. \quad (26)$$

Here κ^q is the contribution of the quark flavor q to the anomalous magnetic moment of the nucleon. The flavor dipole moments for the light quarks in the nucleon are therefore of the order $0.2\, fm$, which is quite significant in comparison to the size of the nucleon. Similarly, in Eq. (23) there are two terms which generate distortions, one is determined by the first derivative of $\mathcal{E}_T + 2\tilde{\mathcal{H}}_T$ and the other is given by the second derivative of $\tilde{\mathcal{H}}_T$. We will see later that the specific form of the relations between GPDs and TMDs depends on the number of the derivatives of the GPDs in impact parameter space.

C. Transverse momentum dependent parton distributions (TMDs)

The quark TMDs are defined through the unintegrated quark-quark correlator for SIDIS [31,32]. The TMDs depend on the longitudinal momentum fraction x of the active quark and the quark transverse momentum $\mathbf{p}_T$. The TMDs provide a three-dimensional view of the parton distributions in momentum space. In a hadronic state $|P, S\rangle$ with momentum P and polarization S, the TMDs can be defined through the quark-quark correlation function as

$$\Phi^{q[\Gamma]}(x, \mathbf{p}_T; \mathbf{S}) = \frac{1}{2} \int \frac{dz^-}{2\pi} \frac{d^2\mathbf{z}_T}{(2\pi)^2} e^{ik\cdot z} \left\langle P; S \middle| \bar{\psi}\left(-\frac{1}{2}z\right) \Gamma \times \mathcal{W}_{\mathrm{TMD}}\left(-\frac{1}{2}z; \frac{1}{2}z\right) \psi\left(\frac{1}{2}z\right) \middle| P; S \right\rangle \Big|_{z^+=0^+}, \quad (27)$$

in which a summation over the color of the quark fields is implicit. In the chosen frame, the nucleon four momentum $P \equiv (P^+, \frac{M^2}{P^+}, \mathbf{0})$, and virtual photon momentum $q \equiv (x_B P^+, \frac{Q^2}{x_B P^+}, \mathbf{0})$, where $x_B = \frac{Q^2}{2P.q}$ is the Bjorken variable and $Q^2 = -q^2$. The covariant spin vector S for the nucleon with helicity λ is defined as $(S^+ = \frac{\lambda P^+}{M}, S^- = -\frac{\lambda P^-}{M}, \mathbf{S}_T)$. The Wilson line in TMD correlators is far more complicated than that in the GPD correlators and is given by [13]

$$\mathcal{W}_{\mathrm{TMD}}\left(-\frac{1}{2}z; \frac{1}{2}z\right)\Big|_{z^+=0^+} = \left[0^+, -\frac{1}{2}z^-, -\frac{1}{2}\mathbf{z}_T; 0^+, +\infty^-, -\frac{1}{2}\mathbf{z}_T\right] \times \left[0^+, +\infty^-, -\frac{1}{2}\mathbf{z}_T; 0^+, +\infty^-, \frac{1}{2}\mathbf{z}_T\right] \times \left[0^+, +\infty^-, \frac{1}{2}\mathbf{z}_T; 0^+, \frac{1}{2}z^-, \frac{1}{2}\mathbf{z}_T\right], \quad (28)$$

where the future pointing Wilson line is running along the positive z^- direction to $+\infty$ for SIDIS, while in the Drell-Yan process the Wilson lines runs along the opposite direction, towards $-\infty$ [33]. The leading twist quark TMDs are obtained from correlator in (27) by using the same three Γ matrices $(\gamma^+, \gamma^+\gamma_5, \sigma^{+j}\gamma_5)$. The corresponding antiquark TMDs can be obtained by the same light-cone correlation functions by using charge conjugated fields. There exist eight leading twist quark TMDs, which are all real valued. Taking $\Gamma = \gamma^+$ in Eq. (27), we get

$$\Phi^q(x, \mathbf{p}_T; S) = \Phi^{q[\gamma^+]}(x, \mathbf{p}_T; S) = f_1^q(x, \mathbf{p}_T^2) - \frac{\epsilon_T^{ij} p_T^i S_T^j}{M} f_{1T}^{\perp q}(x, \mathbf{p}_T^2). \quad (29)$$

f_1^q is the unpolarized quark distribution for a quark flavor q, and $f_{1T}^{\perp q}$ represents the (naive) T-odd Sivers function which appears for a transversely polarized target ($S_T \neq 0$). The Sivers function describes the distribution of the unpolarized quark carrying a longitudinal momentum fraction x and transverse momentum $\mathbf{p}_T$ in a transversely polarized target. If the second term on the right-hand side in (29) is nonzero then the quark TMD correlator Φ^q is not axially symmetric in the $\mathbf{p}_T$ plane, i.e., the distribution becomes distorted. This distortion is supposed to be the origin of various observed single spin asymmetries in hard semi-inclusive reactions [34,35]. Setting $\Gamma = \gamma^+\gamma_5$ and $i\sigma^{j+}\gamma_5$ in Eq. (27), we have

$$\tilde{\Phi}^q(x, \mathbf{p}_T; S) = \Phi^{q[\gamma^+\gamma_5]}(x, \mathbf{p}_T; S) = \lambda g_{1L}^q(x, \mathbf{p}_T^2) + \frac{\mathbf{p}_T \cdot \mathbf{S}_T}{M} g_{1T}^q(x, \mathbf{p}_T^2), \quad (30)$$

$$\Phi_T^{q,j}(x,\mathbf{p}_T;S) = \Phi^{q[i\sigma^{j+}\gamma_5]}(x,\mathbf{p}_T;S)$$
$$= -\frac{\epsilon_T^{ij}\mathbf{p}_T^i}{M} h_1^{\perp q}(x,\mathbf{p}_T^2) + \frac{\lambda \mathbf{p}_T^j}{M} h_{1L}^{\perp q}(x,\mathbf{p}_T^2)$$
$$+ S_T^j \left(h_{1T}^q(x,\mathbf{p}_T^2) + \frac{\mathbf{p}_T^2}{2M^2} h_{1T}^{\perp q}(x,\mathbf{p}_T^2) \right)$$
$$+ \frac{2\mathbf{p}_T^j \mathbf{p}_T\cdot\mathbf{S}_T - S_T^j \mathbf{p}_T^2}{2M^2} h_{1T}^{\perp q}(x,\mathbf{p}_T^2). \quad (31)$$

Here, $h_1^{\perp q}$ is the Boer-Mulders function, which gives the distribution of transversely polarized quarks inside an unpolarized hadron. The process dependence of the Wilson line leads to a sign difference in the T-odd TMDs, e.g., $f_{1T}^{\perp q}|_{SIDIS} = -f_{1T}^{\perp q}|_{DY}$; whereas in hadron-hadron scattering with hadronic final states, even more complicated paths for the Wilson line can arise [36–39]. There are altogether six T-even TMDs and two (Sivers and Boer Mulders) T-odd TMDs. The p_T integrated function of $f_1^\nu(x,p_T^2)$ gives the unpolarized parton distribution $f_1^\nu(x)$ and $g_{1L}^\nu(x,p_T^2)$ gives the helicity distribution $g_{1L}^\nu(x)$. The transversity TMD $h_1^\nu(x,p_T^2)$ is defined as

$$h_1^\nu(x,\mathbf{p}_T^2) = h_{1T}^\nu(x,\mathbf{p}_T^2) + \frac{\mathbf{p}_T^2}{2M^2} h_{1T}^{\perp\nu}(x,\mathbf{p}_T^2), \quad (32)$$

and when integrated over the transverse momentum gives the transversity parton distribution $h_1^\nu(x)$.

Like the p_T integrated TMDs, some GPDs in the limit $\xi = t = 0$, are also related to the twist-2 pdfs. Thus we get some model-independent relations between GPDs and TMDs:

$$f_1^q(x) = \int d^2\mathbf{p}_T f_1^q(x,\mathbf{p}_T^2) = H^q(x,0,0)$$
$$= \int d^2\mathbf{b}_T \mathcal{H}^{q/g}(x,\mathbf{b}_T^2), \quad (33)$$

$$g_1^q(x) = \int d^2\mathbf{p}_T g_{1L}^q(x,\mathbf{p}_T^2) = \tilde{H}^q(x,0,0)$$
$$= \int d^2\mathbf{b}_T \tilde{\mathcal{H}}^q(x,\mathbf{b}_T^2), \quad (34)$$

$$h_1^q(x) = \int d^2\mathbf{p}_T \left(h_{1T}^q(x,\mathbf{p}_T^2) + \frac{\mathbf{p}_T^2}{2M^2} h_{1T}^{\perp q}(x,\mathbf{p}_T^2) \right)$$
$$= H_T^q(x,0,0)$$
$$= \int d^2\mathbf{b}_T \left(\mathcal{H}_T^q(x,\mathbf{b}_T^2) - \frac{\mathbf{b}_T^2}{M^2}\Delta_b \tilde{\mathcal{H}}_T^q(x,\mathbf{b}_T^2) \right). \quad (35)$$

These relations give important constraints on models, and are satisfied in our model. Next, we investigate a few nontrivial model-dependent relations.

IV. MODEL-DEPENDENT RELATIONS BETWEEN GPDs AND TMDs

In [9], all possible model-dependent relations between GPDs and TMDs are systematically studied. The model-independent relations as given in the previous section are called relations of the first kind. There are a few relations in momentum space. There are also model-dependent relations that connect the GPDs to the IPDpdfs or their derivatives in b_T space. These relations are called second, third, and fourth type depending on the number of derivatives present in the relation. In this section, we investigate nontrivial relations between the TMDs and GPDs, as well as some relations between the different TMDs in our model. We also compare LFQDQ model results with the results of two other spectator models, namely, the scalar diquark spectator model of the nucleons [40] and a quark target model treated in perturbative QCD [9].

Incorporating the FSI effect into the wave functions [41], the Sivers $f_{1T}^{\perp q}$ and the Boer- Mulders $h_1^{\perp q}$ functions can be written as

$$f_{1T}^{\perp q}(x,\mathbf{p}_T^2) = \left(C_S^2 N_S^{\nu 2} - \frac{1}{3} C_A^2 N_0^{\nu 2} \right) f^\nu(x,\mathbf{p}_T^2), \quad (36)$$

$$h_1^{\perp q}(x,\mathbf{p}_T^2) = \left(C_S^2 N_S^{\nu 2} + \left(\frac{1}{3} N_0^{\nu 2} + \frac{2}{3} N_1^{\nu 2} \right) C_A^2 \right) f^\nu(x,\mathbf{p}_T^2), \quad (37)$$

where

$$f^\nu(x,\mathbf{p}_T^2) = (-C_F\alpha_s) \times \frac{1}{x} \left[\frac{\mathbf{p}_T^2 + B(x)}{\mathbf{p}_T^2} \right] \log \left[\frac{\mathbf{p}_T^2 + B(x)}{B(x)} \right]$$
$$\times \frac{1}{16\pi^3} A_1^\nu(x) A_2^\nu(x) \exp[-a(x)\mathbf{p}_T^2], \quad (38)$$

and where $B(x)$ and $a(x)$ are defined in Eqs. (9) and (12), respectively, and $C_A = C_V(C_{VV})$ for $u(d)$ quark. In the final state interactions, gluon exchange strength $\frac{e_1 e_2}{4\pi} \to -C_F\alpha_s$, while the pretzelosity $h_{1T}^{\perp q}$ TMDs can be written as [21]

$$h_{1T}^{\nu\perp}(x,\mathbf{p}_T^2) = -\left(C_S^2 N_S^{\nu 2} - C_V^2 \frac{1}{3} N_0^{\nu 2} \right) \frac{2\ln(1/x)}{\pi\kappa^2}$$
$$\times x^{2a_2^\nu - 2}(1-x)^{2b_2^\nu - 1} \exp\left[-a(x)\mathbf{p}_T^2\right], \quad (39)$$

and are found to satisfy the inequality relation [16]

$$|h_1^\perp(x,\mathbf{p}_T^2)| > |f_{1T}^\perp(x,\mathbf{p}_T^2)|. \quad (40)$$

From Eqs. (36) and (37), we can easily check that the Boer-Mulders function is proportional to the Sivers function. The Boer-Mulders function can be parametrized [16,42] as

$$h_1^{\perp\nu}(x,\mathbf{p}_T^2) = \lambda^\nu f_{1T}^{\perp\nu}(x,\mathbf{p}_T^2), \tag{41}$$

where

$$\lambda^\nu = \frac{(C_S^2 N_S^{\nu 2} + (\frac{1}{3}N_0^{\nu 2} + \frac{2}{3}N_1^{\nu 2})C_A^2)}{(C_S^2 N_S^{\nu 2} - \frac{1}{3}C_A^2 N_0^{\nu 2})}. \tag{42}$$

Putting in the model parameters in Eq. (42), we get $\lambda^u = 2.29$ and $\lambda^d = -1.08$. Since the Sivers function is negative for up quarks and positive for down quarks, from the above expression [Eq. (41)] we can conclude that the Boer-Mulders function is negative for both up and down quarks.

A. Moment relations between GPDs and TMDs in momentum space

The n^{th} moment of the GPD X is defined as

$$X^{(n)}(x) = \frac{1}{2M^2}\int d^2\mathbf{\Delta}_T \left(\frac{\mathbf{\Delta}_T^2}{2M^2}\right)^{n-1} X\left(x, 0, -\frac{\mathbf{\Delta}_T^2}{(1-x)^2}\right), \tag{43}$$

and similarly the moment of the TMD Y is defined as

$$Y^{(n)}(x) = \int d^2\mathbf{p}_T \left(\frac{\mathbf{p}_T^2}{2M^2}\right)^n Y(x,\mathbf{p}_T^2). \tag{44}$$

The moments for GPD E^q and $(E_T^q + 2\tilde{H}_T^q)$ are obtained as

$$E^{q(n)}(x) = -\left(C_s^2 N_s^2 - \frac{1}{3}C_A^2 N_0^{\nu 2}\right)\pi 2^{n+1}\left(\frac{1}{M^2}\right)^n \Gamma(n) \times x^{a_1^\nu + a_2^\nu - 1}(1-x)^{b_1^\nu + b_2^\nu + 2}\left(\frac{\log(1/x)}{\kappa^2(x-1)^4}\right)^{-n}, \tag{45}$$

and

$$E_T^{q(n)}(x) + 2\tilde{H}_T^{q(n)}(x) = \left(C_s^2 N_s^2 + C_A^2\left(\frac{1}{3}N_0^{\nu 2} + \frac{2}{3}N_1^{\nu 2}\right)\right)\pi 2^n\left(\frac{1}{M^2}\right)^n \Gamma(n) \times x^{a_1^\nu + a_2^\nu - 1}(1-x)^{b_1^\nu + b_2^\nu + 2}\left(\frac{\log(1/x)}{\kappa^2(x-1)^4}\right)^{-n}. \tag{46}$$

The analytic form of the moments for Sivers and Boer-Mulders functions are too complicated and lengthy to present here. The moment relation between Sivers function and GPD E^q in the scalar diquark model was obtained in [9] and has the general form

$$f_{1T}^{\perp q(n)}(x) = -\frac{g^2 e_q e_s (1-x)}{16(2\pi)^2}\frac{(m_q + xM)\tilde{M}^{2n-2}(x) H_{-n}}{2^n M^{2n-1}\sin(n\pi)} = -\frac{e_q e_s}{2(2\pi)^2(1-x)}\frac{H_{-n}\Gamma(2-2n)}{\Gamma^2(1-n)}E^{q(n)}(x). \tag{47}$$

The relation given by Eq. (47) generally holds for $0 \le n \le 1$, i.e., n is not necessarily an integer where H_n is the analytic continuation of the harmonic number for noninteger n. In the LFQDQ model, it is not possible to obtain a similar relation analytically for a general value of n, however, relations similar to Eq. (47) can be derived in the scalar diquark model [9] for three particular values of n, as

$$f_{1T}^{\perp q(0)}(x) = \frac{\pi e_q e_s}{48(1-x)}E^q(x,0,0), \tag{48}$$

$$f_{1T}^{\perp q(1/2)}(x) = \frac{2e_q e_s \ln(2)}{(2\pi)^3(1-x)}E^{q(1/2)}(x), \tag{49}$$

$$f_{1T}^{\perp q(1)}(x) = \frac{e_q e_s}{4(2\pi)^2(1-x)}E^{q(1)}(x), \tag{50}$$

the moment relations for the Sivers function, $f_{1T}^{\perp q}$, and the corresponding GPD E^q in the LFQDQ model are evaluated numerically and the results for the up quarks are compared with scalar diquark model results in Fig. 1. It is seen from the plot that the zeroth moment of the Sivers function in both models obey the same relation for $x > 0.5$; although the qualitative behavior for the next two moments ($n = 1/2, 1$) are similar, they do not match except for a narrow range roughly in the region $0.1 < x < 0.5$. Furthermore, in the LFQDQ model, a kink appears at around $x = 0.05$. This is due to that fact that both the functions $f_{1T}^{\perp q}(x)$ and the GPD $E^q(x)$ have maxima at the same x. The other T-odd TMD, i.e., Boer-Mulders function and the corresponding GPD, also show similar behavior, which can be seen in Fig. 2.

In the LFQDQ model, the relations between the pretzelosity, $h_{1T}^{\perp q}$, and the GPD, $\tilde{H}_T^q$, can be given analytically. By using Eqs. (43) and (44), the n^{th} moment of the pretzelosity TMD, $h_{1T}^{\perp q(n)}$, and the n^{th} moment of the corresponding GPD, $\tilde{H}_T^{q(n)}$, is given as

$$h_{1T}^{\perp q(n)}(x) = -\left(C_s^2 N_s^2 - \frac{1}{3}C_A^2 N_0^{\nu 2}\right)\frac{2^{1-n}}{\kappa^2}\left(\frac{1}{M^2}\right)^n \times \Gamma(n+1)x^{2a_2^\nu - 2}(1-x)^{2b_2^\nu - 2} \times \log\left(\frac{1}{x}\right)a(x)^{-n-1} \tag{51}$$

$$\tilde{H}_T^{q(n)}(x) = \left(C_s^2 N_s^2 - \frac{1}{3}C_A^2 N_0^{\nu 2}\right)\pi 2^n x^{2a_2^\nu - 2}(1-x)^{2b_2^\nu + 3} \times \left(\frac{1}{M^2}\right)^n \Gamma(n)a(x)^{-n}, \tag{52}$$

and they satisfy the relation

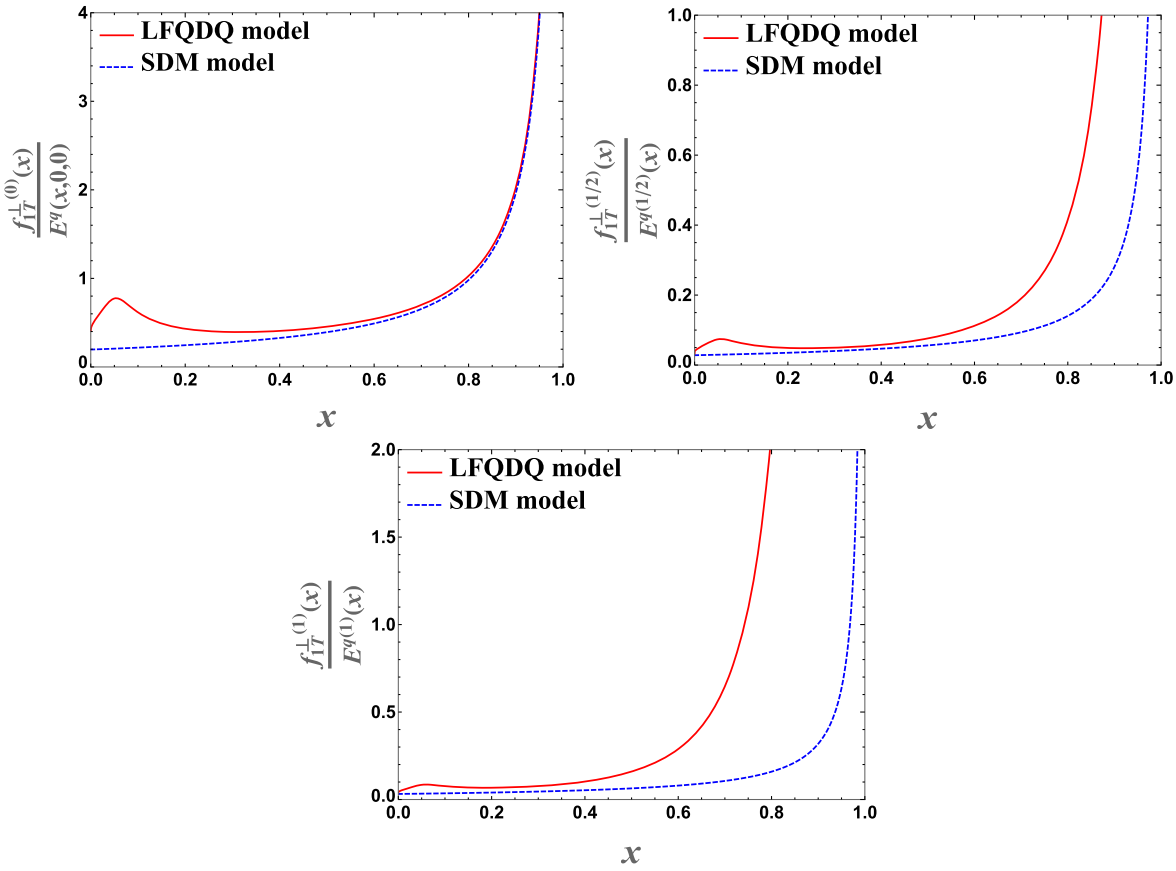

FIG. 1. The left plot is corresponding the ratio of the zeroth moment of the Sivers TMD for the up quarks $f_{1T}^{\perp u(0)}(\mathrm{x})$ to the corresponding GPD $E^u(x,0,0)$. The right plot is for the ratio of $f_{1T}^{\perp u(1/2)}(x)$ to $E^{u(1/2)}(x)$, and the lower plot is for the ratio of $f_{1T}^{\perp u(1)}(x)$ to $E^{u(1)}(x)$.

$$h_{1T}^{\perp q(n)} = \frac{2^{1-2n}\Gamma(n+1)}{\pi(1-x)^2\Gamma(n)}\tilde{H}_T^{q(n)}(x), \tag{53}$$

which holds for $0 \le n \le 1$. Note that this relation is the same with or without the axial-vector diquark in the model. The explicit forms of the relation in Eq. (53) for three different values of n are as follows:

$$h_{1T}^{\perp q(0)}(x) = \frac{2}{(1-x)^2}\tilde{H}_T^{q}(x,0,0), \tag{54}$$

$$h_{1T}^{\perp q(1/2)}(x) = \frac{1}{2\pi(1-x)^2}\tilde{H}_T^{q(1/2)}(x), \tag{55}$$

$$h_{1T}^{\perp q(1)}(x) = \frac{1}{2\pi(1-x)^2}\tilde{H}_T^{q(1)}(x). \tag{56}$$

These relations can be compared with the corresponding relations in the scalar diquark model and quark target models, which are given by [9]

$$h_{1T}^{\perp q(0)}(x) = \frac{3}{(1-x)^2}\tilde{H}_T^{q}(x,0,0), \tag{57}$$

$$h_{1T}^{\perp q(1/2)}(x) = \frac{8}{(2\pi)^2(1-x)^2}\tilde{H}_T^{q(1/2)}(x), \tag{58}$$

$$h_{1T}^{\perp q(1)}(x) = \frac{1}{2\pi(1-x)^2}\tilde{H}_T^{q(1)}(x). \tag{59}$$

Note that Eq. (56) exactly matches with Eq. (59), and the other two relations (Eqs. (54) and (55) have similar structure to Eqs. (57) and (58), except the constant factors, which may be model dependent. The ratios of $h_{1T}^{\perp q(n)}(x)$ and $\tilde{H}_T^{q(n)}(x)$ for $0 \le n \le 1$ go as $1/(1-x)^2$ in the scalar diquark model considered in [9], as well as in our model with or without the axial-vector diquark. It needs to be investigated whether this is true in any diquark-type model.

The general structure of the relations in Eqs. (48)–(50), and the relations in Eqs. (54)–(56), is not same due to the FSI contribution to the T-odd TMDs, like the Sivers and Boer-Mulders functions. The pretzelosity distribution is a T-even quantity and at the level of one gluon exchange does

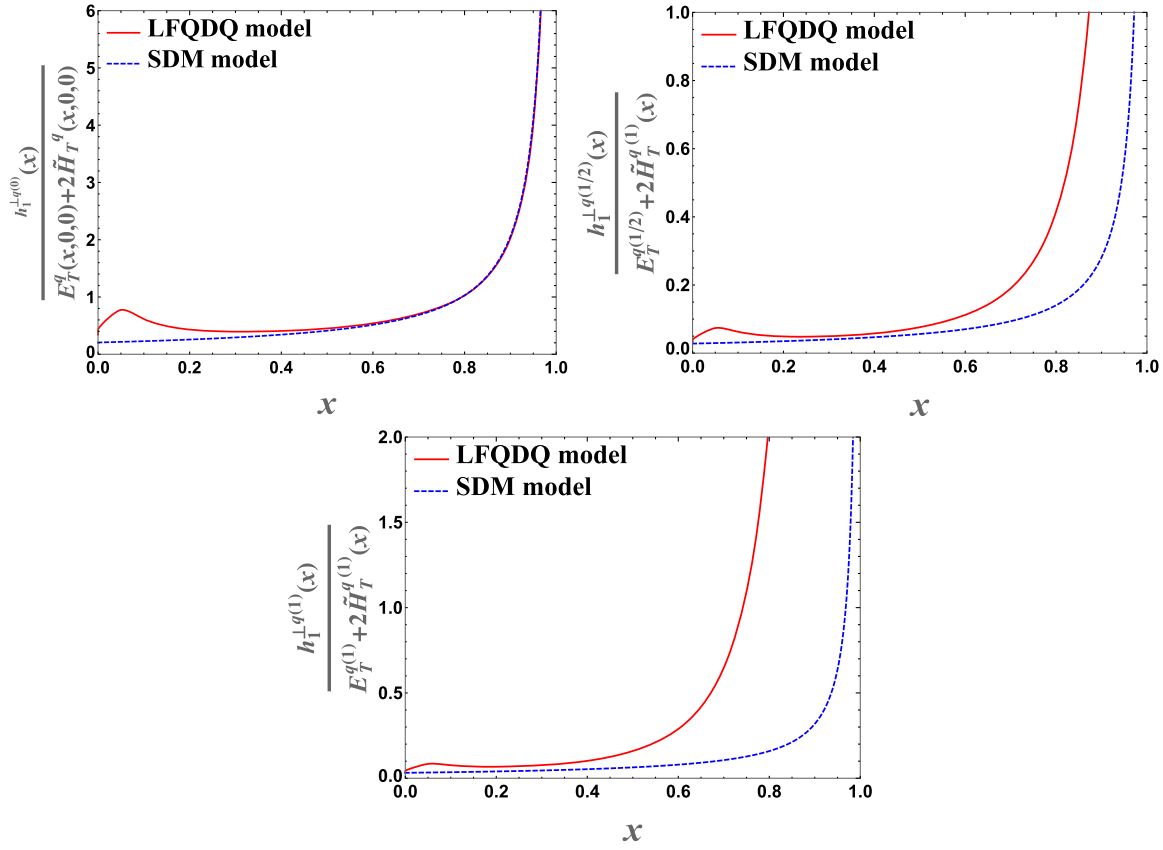

FIG. 2. The left plot is corresponding the ratio of the zeroth moment of Boer-Mulders TMD for the up quarks $h_1^{\perp u(0)}(\mathrm{x})$ to the corresponding GPD, $E_T^u(x,0,0)+2\tilde{H}_T^u(x,0,0)$. The right one is for the ratio of the $h_1^{\perp q(1/2)}(x)$ to $E_T^{u(1/2)}(x)+2\tilde{H}_T^{u(1/2)}(x)$, and the lower one is for the ratio of the $h_1^{\perp q(1)}(x)$ to $E_T^{u(1)}(x)+2\tilde{H}_T^{u(1)}(x)$.

not receive contribution from the Wilson line. For this reason, coupling constants appear in the relations involving T-odd TMDs. Also the relative power of $(1-x)$ between the moments of the TMDs and of GPDs differs in these two types of relations. In Fig. 3 we have compared LFQDQ results in Eqs. (54)–(56) to the scalar diquark model results in Eqs. (57)–(59).

The n^{th} moment of the GPD $\tilde{H}_T^q$ can be written in terms of the second derivative of the impact parameter distribution $\tilde{\mathcal{H}}_T^q$ [9]. Here we consider $n=1$ to have

$$\begin{aligned}&\int d^2\mathbf{b}_T \frac{\mathbf{b}_T^2}{2M^2} 2(\tilde{\mathcal{H}}_T^q(x,\mathbf{b}_T^2))''\\&= -\pi\int_0^\infty db_T^2 \frac{1}{2M^2} 2(\tilde{\mathcal{H}}_T^q(x,\mathbf{b}_T^2))'\\&= \frac{\pi}{M^2}\tilde{\mathcal{H}}_T^q(x,0)\\&= \frac{1}{(2\pi)(1-x)^2}\tilde{H}_T^{q(1)}(x). \end{aligned} \tag{60}$$

In the above equation we take the Fourier transform of GPD $\tilde{H}_T^q(x,t)$ and perform the integration by parts. Then we arrive at the relation

$$\begin{aligned}h_{1T}^{\perp q(1)}(x) &= \int d^2\mathbf{p}_T \frac{\mathbf{p}_T^2}{2M^2} h_{1T}^{\perp q}(x,\mathbf{p}_T^2)\\&= \int d^2\mathbf{b}_T \frac{\mathbf{b}_T^2}{2M^2} 2(\tilde{\mathcal{H}}_T^q(x,\mathbf{b}_T^2))''. \end{aligned} \tag{61}$$

This relation is also valid for both the scalar diquark model and quark target model [9].

B. Lensing function

In [28], a nontrivial model-dependent relation was found between GPD E^q in impact parameter space and the Sivers function $f_{1T}^{\perp q}$. The average transverse momentum of an unpolarized quark in a transversely polarized target [43] is defined by

$$\begin{aligned}\langle p_T^{q,i}(x)\rangle_{UT} &= \int d^2\mathbf{p}_T p_T^i \Phi^q(x,\mathbf{p}_T;S)\\&= -\int d^2\mathbf{p}_T p_T^i \frac{\epsilon_T^{jk} p_T^j S_T^k}{M} f_{1T}^{\perp q}(x,\mathbf{p}_T^2) \end{aligned} \tag{62}$$

$$\simeq \int d^2\mathbf{b}_T \mathcal{I}^{q,i}(x,\mathbf{b}_T)\frac{\epsilon_T^{jk} b_T^j S_T^k}{M}(\mathcal{E}^q(x,\mathbf{b}_T^2))'. \tag{63}$$

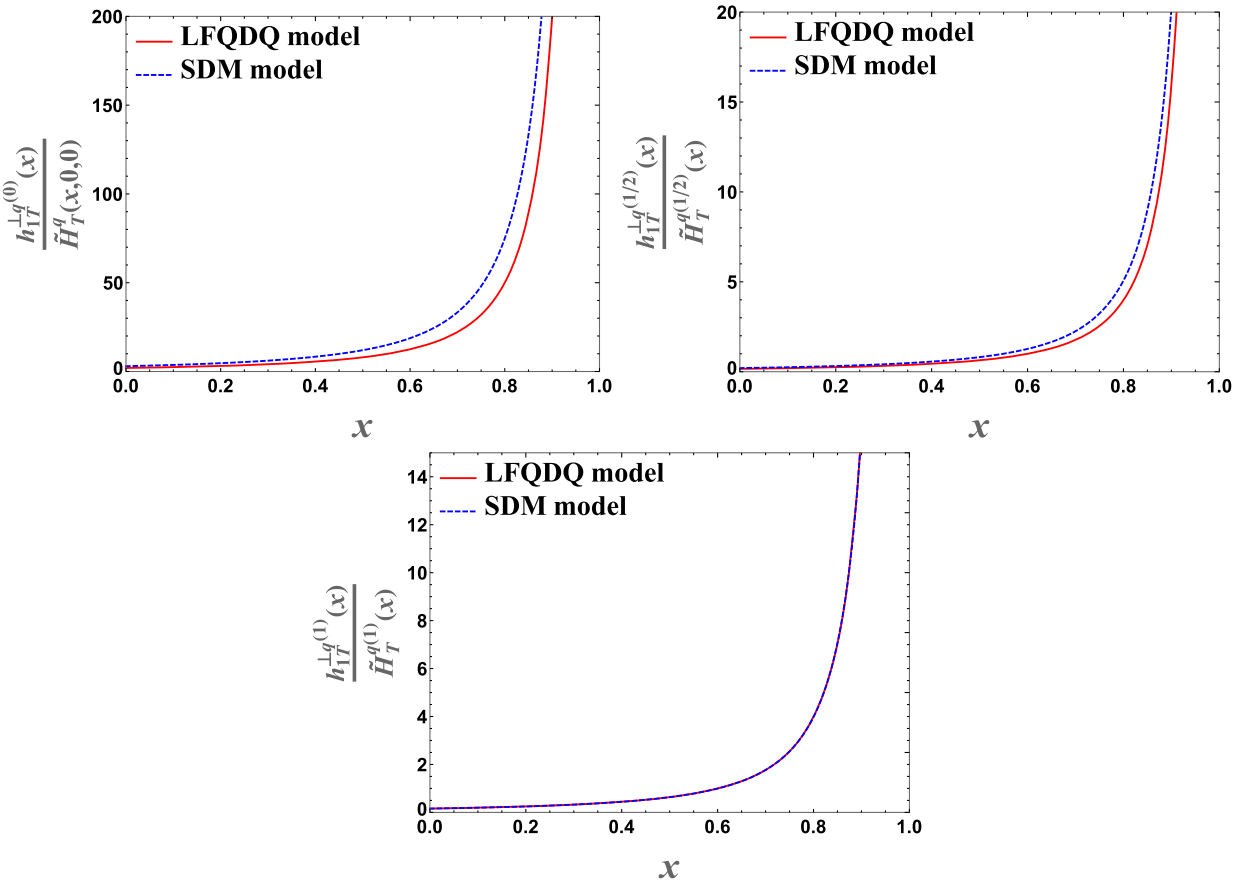

FIG. 3. The left plot is corresponding to the ratio of the zeroth moment of pretzelosity TMD $[h_{1T}^{\perp u(0)}(x)]$ to the corresponding GPD, $\tilde{H}_T^u(x,0,0)$. The right plot is the ratio of $h_{1T}^{\perp u(1/2)}(x)$ to $\tilde{H}_T^{u(1/2)}(x)$, and the lower one is the ratio of $h_{1T}^{\perp u(1)}(x)$ to $\tilde{H}_T^{u(1/2)}(x)$.

The above relation (63) is applicable in models where the nucleon state is approximated as an effective two-particle bound state like a diquark model and at the level of one gluon exchange [44]; however it is found to be not valid when vector and axial-vector diquarks are included [10]. Here $\mathcal{I}^{q,i}$ contains the effect of the FSI, i.e., the one gluon exchange in the final state between the active quark and the spectator system. In such models, Eq. (63) provides the intuitive understanding of the origin of the Sivers transverse SSA.

However, in general, the average transverse momentum $\langle p_T^{q,i}(x)\rangle_{UT}$ caused by the Sivers effect can not be factorized into the lensing function $\mathcal{I}^{q,i}$ and the distortion of the impact parameter distribution of quarks in a transversely polarized target which is determined by $(\mathcal{E}^q)'$. So, the relation (63) is model dependent and no model-independent relation has been established between the Sivers function $f_{1T}^{\perp q}$ and GPD E^q. In our model we have scalar as well as vector and axial-vector diquark contributions. One can still obtain a relation connecting the Sivers function to a distortion of the GPD E^q in impact parameter space by using an ansatz for the lensing function and obtaining a fit. Two different analytic forms of the function are needed for the low-x and high-x regions. In the lower x region, $0 < x < 0.2$, we got the expression for the lensing function as

$$\mathcal{I}^{q,i}(x,\mathbf{b}_T) = \frac{5C_F\alpha_S}{2\pi}x^{3/2}(1-x)^{-1/5}\log^5\left(\frac{1}{x}\right)\frac{b_T^i}{\mathbf{b}_T{}^2}, \quad (64)$$

and for the higher x region, i.e., in the region $0.2 < x < 1$, the lensing function takes the form

$$\mathcal{I}^{q,i}(x,\mathbf{b}_T) = \frac{2C_F\alpha_S}{\pi}\sqrt{(1-x)}\log\left(\frac{1}{x}\right)\frac{b_T^i}{\mathbf{b}_T{}^2}. \quad (65)$$

The lensing function is model dependent but does not depend on the parton type. The corresponding plots for the Eq. (63) by using Eqs. (64) and (65) are shown in Fig. 4. The lensing function in the scalar diquark model is relatively easier to extract and is valid for the whole range of $x(0 < x < 1)$:

$$\mathcal{I}^{q,i}_{SDM}(x,\mathbf{b}_T) = \frac{5}{\pi}(C_F\alpha_S)(1-x)\frac{b_T^i}{b_T^2}. \quad (66)$$

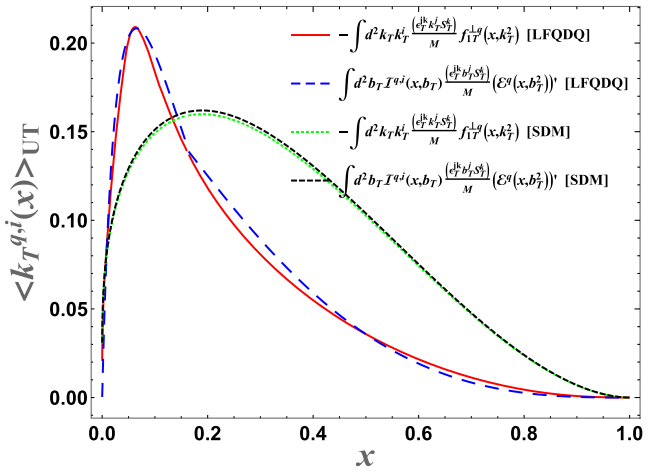

FIG. 4. Lensing function obtained from the Sivers function. The average transverse momentum evaluated using Sivers function [Eq. (62)] and lensing function [Eq. (63)] are shown for LFQDQ and SDM models. For the LFQDQ model, the lensing function is given in Eqs. (64) and (65), while the lensing function for the SDM model is given in Eq. (66).

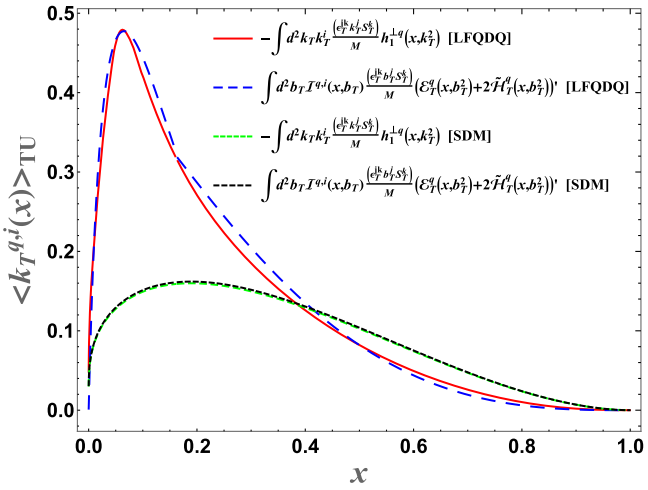

FIG. 5. Lensing function for Boer-Mulders function. The average transverse momentum evaluated using Boer-Mulders function and lensing function are shown for the LFQDQ and SDM models. For the LFQDQ model, the lensing function is given in Eqs. (64) and (65), while the lensing function for the SDM model is given in Eq. (66).

In Fig. 4, the results for the scalar diquark model are also shown. The momentum distributions in the two models are not the same; in the scalar diquark model, the distribution peaks at around $x \sim 0.2$ while inclusion of the axial diquark enhances the diquark contribution and shifts the peak towards the lower x.

The average transverse momentum $\langle p_T^{q,i}(x)\rangle_{TU}^{j}$ of a transversely polarized quark (with polarization along j-direction) in an unpolarized nucleon can be expressed in terms of the Boer-Mulders function which is again related with the GPDs [44,45],

$$\langle p_T^{q,i}(x)\rangle_{TU}^{j} = \int d^2\mathbf{p}_T p_T^i \Phi^{q,j}(x,\mathbf{p}_T;S) = -\int d^2\mathbf{p}_T p_T^i \frac{\epsilon_T^{kj} p_T^k}{M} h_1^{\perp q}(x,\mathbf{p}_T^2) \tag{67}$$

$$= \int d^2\mathbf{b}_T \mathcal{I}_{\mathrm{SDM}}^{q,i}(x,\mathbf{b}_T)\frac{\epsilon_T^{kj} b_T^k}{M} \times (\mathcal{E}_T^q(x,\mathbf{b}_T^2) + 2\tilde{\mathcal{H}}_T^q(x,\mathbf{b}_T^2))'. \tag{68}$$

The Sivers and Boer Mulder's TMDs are the same in this model except the normalization constant and corresponding GPD $E_T^q + 2\tilde{H}_T^q$ also has the same structure as the GPD E^q. The lensing function is also exactly the same as quarks Sivers effect, which means that it is not only independent of the parton type but also of its polarization. The magnitude of the Boer-Mulder function is directly proportional to the distortion of the impact parameter distribution of the transversely polarized quarks inside an unpolarized nucleon [46]. The distortion can be given by the first derivative of $\mathcal{E}_T^q(x,\mathbf{b}_T^2) + 2\tilde{\mathcal{H}}_T^q(x,\mathbf{b}_T^2)$. The corresponding plots for Eqs. (67) and (68) by using Eqs. (64) and (65) for the LFQDQ model and Eq. (66) for the SDM model are shown in Fig. 5.

V. RELATIONS AMONG TMDs

The TMDs are found to satisfy many interesting model-dependent relations. Many such relations have been found for the scalar diquark model [47]. Though the scalar diquark model satisfies the saturation limit of the Soffer bound, with inclusion of the axial-vector diquark, the inequality relation of the Soffer bound is satisfied:

$$h_1^{q(s)}(x,p_T^2) < \frac{1}{2}(f_1^{q(s)}(x,p_T^2) + g_1^{q(s)}(x,p_T^2)). \tag{69}$$

The ratio of $g_{1T}^{q(s)}(x,p_T^2)$ and $h_1^{q(s)}(x,p_T^2)$ is found to be independent of transverse momentum p_T:

$$\frac{g_{1T}^{q(s)}(x,p_T^2)}{h_1^{q(s)}(x,p_T^2)} = \mathcal{J}(x) = 2x^{a_2^\nu - a_1^\nu - 1}(1-x)^{b_1^\nu - b_2^\nu}. \tag{70}$$

The two nonlinear relations which connect T-even chirally odd leading twist TMDs in the scalar diquark model [47,48] are

$$(g_{1T}^{q(s)}(x,p_T^2))^2 + 2h_1^{q(s)}(x,p_T^2)h_{1T}^{\perp q(s)}(x,p_T^2) = 0, \tag{71}$$

$$h_1^{q(s)}(x,p_T^2)h_{1T}^{\perp q(s)}(x,p_T^2) = -\frac{1}{2}[h_{1L}^{q(s)\perp}(x,p_T^2)]^2. \tag{72}$$

Eq. (72) implies that $h_1^{q(s)}$ and $h_{1T}^{q(s)}$ must have opposite signs. The relations with axial-vector diquarks are more involved compared to the relations in the scalar diquark model. The relations in Eqs. (71) and (72) have been shown to be a consequence of spherical symmetry [48]. The corresponding relations with the axial-vector diquark are

$$(g_{1T}^{q(A)}(x,p_T^2))^2 + 2h_1^{q(A)}(x,p_T^2)h_{1T}^{\perp q(A)}(x,p_T^2) = 0 \quad (73)$$

$$[h_{1L}^{\perp q(A)}(x,p_T^2)]^2 = -\lambda_1^q h_1^{q(A)}(x,p_T^2)h_{1T}^{\perp q(A)}(x,p_T^2), \quad (74)$$

where the proportionality constant $\lambda_1^q = \frac{(N_0^{\nu 2}-2N_1^{q2})^2}{N_0^{q4}} > 0$ and the similar conclusion about the opposite polarity of $h_1^{q(s)}$ and $h_{1T}^{q(s)}$ holds. Two more interesting relations with the axial-vector diquark are

$$g_{1T}^{q(A)}(x,p_T^2) = \frac{N_0^{q2}}{N_0^{q2}+2N_1^{q2}} h_{1L}^{\perp q(A)}(x,p_T^2)$$
$$\Rightarrow g_{1T}^{q(A)}(x,p_T^2) < h_{1L}^{\perp q(A)}(x,p_T^2), \quad (75)$$

$$\frac{p_T^2}{2M^2} h_{1T}^{\perp q(A)}(x,p_T^2) = h_1^{q(A)}(x,p_T^2) - h_{1T}^{q(A)}(x,p_T^2). \quad (76)$$

The relations among the TMDs for the full LFQDQ model (scalar diquark + axial-vector diquark model) can be given as

$$g_{1T}^q(x,p_T^2) = \lambda_1^q h_{1L}^{\perp q}(x,p_T^2) \quad (77)$$

$$g_{1T}^q(x,p_T^2) = [2x^{(-a_1^q+a_2^q-1)}(1-x)^{(-b_1^q+b_2^q)}]h_1^q(x,p_T^2) \quad (78)$$

$$h_{1T}^q(x,p_T^2) = \lambda_2^q f_1^q(x,p_T^2) \quad (79)$$

$$h_{1T}^q(x,p_T^2) + \frac{p_T^2}{2M^2} h_{1T}^{\perp q}(x,p_T^2) = h_1^q(x,p_T^2) \quad (80)$$

$$(g_{1T}^q(x,p_T^2))^2 + 2h_1^q(x,p_T^2)h_{1T}^{\perp q}(x,p_T^2) = 0 \quad (81)$$

$$(h_{1L}^{\perp q}(x,p_T^2))^2 = -\lambda_3^q h_1^q(x,p_T^2)h_{1T}^{\perp q}(x,p_T^2), \quad (82)$$

where $\lambda_1^q = \frac{C_v^2 N_0^{q2} - 3C_s^2 N_s^2}{3C_s^2 N_s^2 + C_v^2(N_0^{q2}-2N_1^{q2})}$, and where substituting the parameter values we have $\lambda_1^u = 0.48, \lambda_1^d = 1.08$, $\lambda_2^q = \frac{3C_s^2 N_s^2 - C_v^2 N_0^{q2}}{3C_s^2 N_s^2 + C_v^2(N_0^{q2}+2N_1^{q2})}$. The values of the constant $\lambda_2^u = 0.44$, $\lambda_2^d = -0.93$ imply that for d-quark $h_{1T}^d(x,p_T^2)$ is of opposite sign of $f_1^d(x,p_T^2)$ and $\lambda_3^q = 2\frac{[3C_s^2 N_s^2 + C_A^2(N_0^{q2}-2N_1^{q2})]^2}{[3C_s^2 N_s^2 - C_A^2 N_0^{q2}]^2}$, giving $\lambda_3^u = 8.55$ and $\lambda_3^d = 1.71$. Similarly the simple relations among the T-odd (Sivers and Boer-Mulders) TMDs in the scalar diquark model,

$$h_1^{\perp q(s)}(x,p_T^2) = f_{1T}^{\perp q(s)}(x,p_T^2), \quad (83)$$

translates into the relation in the scalar and axial-vector diquark model as [Eq. (41)]

$$h_1^{\perp q}(x,p_T^2) = \lambda^q f_{1T}^{\perp q}(x,p_T^2), \quad (84)$$

where $\lambda^q = \frac{(C_S^2 N_S^{q2} + (\frac{1}{3}N_0^{q2} + \frac{2}{3}N_1^{q2})C_A^2)}{(C_S^2 N_S^{q2} - \frac{1}{3}C_A^2 N_0^{q2})}, \lambda^u = 2.29, \lambda^d = -1.08.$ Note that for only the scalar diquark, the Sivers and the Boer-Mulders functions are the same which changes when axial-vector diquarks are included.

VI. QUARK ORBITAL ANGULAR MOMENTUM IN A PROTON

The orbital angular momentum (OAM) of a quark inside the nucleon plays an important role in the spin sum rule of the nucleon [49]. One can extract the total quark contribution to the nucleon spin from the combination of the GPDs using Ji's sum rules as

$$L_z^q = \frac{1}{2}\int dx x[H^q(x,0,0) + E^q(x,0,0)] \quad (85)$$

by subtracting the half of the axial charge $\Delta q = \int dx \tilde{H}^q(x,0,0)$ which has the physical interpretation as the spin contribution of quarks with flavor q to the nucleon spin. We can extract the orbital angular momentum of the quark as [50]

$$L_z^q = \frac{1}{2}\int dx[x(H^q(x,0,0) + E^q(x,0,0)) - \tilde{H}^q(x,0,0)], \quad (86)$$

where $H^q(x,\xi,t)$ and $E^q(x,\xi,t)$ are unpolarized GPDs and $\tilde{H}^q(x,\xi,t)$ is the helicity dependent GPD. GPDs H^q, $\tilde{H}^q$, and E^q respectively in the LFQDQ model can be given as

$$H^\nu(x,0,t) = \left(C_s^2 N_s^2 + C_A^2\left(\frac{N_0^{\nu 2}}{3} + \frac{2}{3}N_1^{\nu 2}\right)\right)\left(x^{2a_1^\nu}(1-x)^{2b_1^\nu+1} + \frac{\kappa^2}{M^2\log(x)}x^{2a_2^\nu-2}(1-x)^{2b_2^\nu+3}\right)$$
$$\times\left(1 - \frac{|t|}{4\kappa^2}\log(1/x)\right)\exp\left[-\frac{|t|}{4\kappa^2}\log(1/x)\right], \quad (87)$$

$$\tilde{H}^q(x,0,t) = \left(C_s^2 N_s^2 + C_A^2\left(\frac{N_0^{\nu 2}}{3} - \frac{2}{3}N_1^{\nu 2}\right)\right)\left(x^{2a_1^\nu}(1-x)^{2b_1^\nu+1} - \frac{\kappa^2}{M^2\log(x)}x^{2a_2^\nu-2}(1-x)^{2b_2^\nu+3}\right)$$
$$\times\left(1-\frac{|t|}{4\kappa^2}\log(1/x)\right)\exp\left[-\frac{|t|}{4\kappa^2}\log(1/x)\right], \tag{88}$$

$$E^q(x,0,t) = 2\left(C_s^2 N_s^2 - \frac{1}{3}C_A^2 N_0^{\nu 2}\right)x^{a_1^\nu+a_2^\nu-1}(1-x)^{b_1^\nu+b_2^\nu+2}\exp\left[-\frac{|t|}{4\kappa^2}\log(1/x)\right]. \tag{89}$$

The OAM expressed in terms of the GPDs is usually called the kinetic OAM. Wigner distributions also contain the full correlation between the quark transverse position and three momentum and one can express the orbital angular momentum in terms of the Wigner distribution. This is known as the canonical OAM. The average quark OAM in a nucleon polarized in the z direction can be written as

$$\hat{\ell}_z^\nu(b^-,\mathbf{b}_T,p^+,\mathbf{p}_T) = \frac{1}{4}\int\frac{dz^-d^2\mathbf{z}_T}{(2\pi)^3}e^{-ip\cdot z}\bar{\psi}^\nu(b^-,\mathbf{b}_T)\gamma^+(\mathbf{b}_T\times(-i\partial_T))\psi^\nu(b^--z^-,\mathbf{b}_T). \tag{90}$$

The OAM density operator can be expressed in terms of the Wigner correlator as

$$\hat{\ell}_z^\nu = (\mathbf{b}_T\times\mathbf{p}_T)\hat{W}^{\nu[\gamma^+]}. \tag{91}$$

Thus, in the light-front gauge, the average canonical OAM for the quark is written in terms of Wigner distributions as

$$\ell_z^\nu = \int\frac{d\Delta^+d^2\Delta_T}{2P^+(2\pi)^3}\langle P'';S|\hat{\ell}_z^\nu|P';S\rangle = \int dxd^2\mathbf{p}_Td^2\mathbf{b}_T(\mathbf{b}_T\times\mathbf{p}_T)_z\rho^{\nu[\gamma^+]}(\mathbf{b}_T,\mathbf{p}_T,x,\hat{S}_z). \tag{92}$$

The distribution $\rho^{\nu[\gamma^+]}(\mathbf{b}_T,\mathbf{p}_T,x,\hat{S}_z)$ can be written as [5]

$$\rho^{\nu[\gamma^+]}(\mathbf{b}_T,\mathbf{p}_T,x,+\hat{S}_z) = \rho_{\mathrm{UU}}^\nu(\mathbf{b}_T,\mathbf{p}_T,x) + \rho_{\mathrm{LU}}^\nu(\mathbf{b}_T,\mathbf{p}_T,x), \tag{93}$$

where ρ_{UU} is the Wigner distribution of an unpolarized quark in an unpolarized nucleon, and ρ_{LU} is the Wigner distribution of an unpolarized quark in a longitudinally polarized nucleon. Thus, Eq. (92) can be decomposed into two parts. The term involving ρ_{UU} gives zero:

$$\int dxd^2\mathbf{p}_Td^2\mathbf{b}_T(\mathbf{b}_T\times\mathbf{p}_T)_z\rho_{\mathrm{UU}}^\nu(\mathbf{b}_T,\mathbf{p}_T,x) = 0, \tag{94}$$

which implies that in an unpolarized nucleon there is no net quark OAM; while the other part can be related to the twist-2 quark canonical OAM in light-front gauge and can be written in terms of GTMDs as

$$\ell_z^\nu = -\int dxd^2\mathbf{p}_T\frac{\mathbf{p}_T^2}{M^2}F_{1,4}^\nu(x,0,\mathbf{p}_T^2,0,0). \tag{95}$$

The correlation between the proton spin and quark canonical OAM can be understood from ℓ_z^ν. If $\ell_z^\nu > 0$, it means the quark OAM is parallel to the proton spin, and if $\ell_z^q < 0$, then the quark OAM is antiparallel to the proton spin. In the LFQDQ model the GTMD $F_{1,4}^\nu(x,0,\mathbf{p}_T^2,0,0)$ can be given as

$$F_{1,4}^\nu(x,0,\mathbf{p}_T^2,0,0) = -\left(C_S^2N_S^2 + C_V^2\left(\frac{1}{3}N_0^2 - \frac{2}{3}N_1^2\right)\right)^\nu\frac{1}{16\pi^3}\frac{(1-x)}{x^2}|A_2^\nu(x)|^2\exp[-a(x)\mathbf{p}_T^2], \tag{96}$$

and by using Eq. (95) the canonical OAM can be written as

$$\ell_z^\nu(x) = \left(C_S^2N_S^2 + C_V^2\left(\frac{1}{3}N_0^2 - \frac{2}{3}N_1^2\right)\right)^\nu\frac{\kappa^2}{M^2\log(1/x)}x^{2a_2^\nu-2}(1-x)^{2b_2^\nu+4} \tag{97}$$

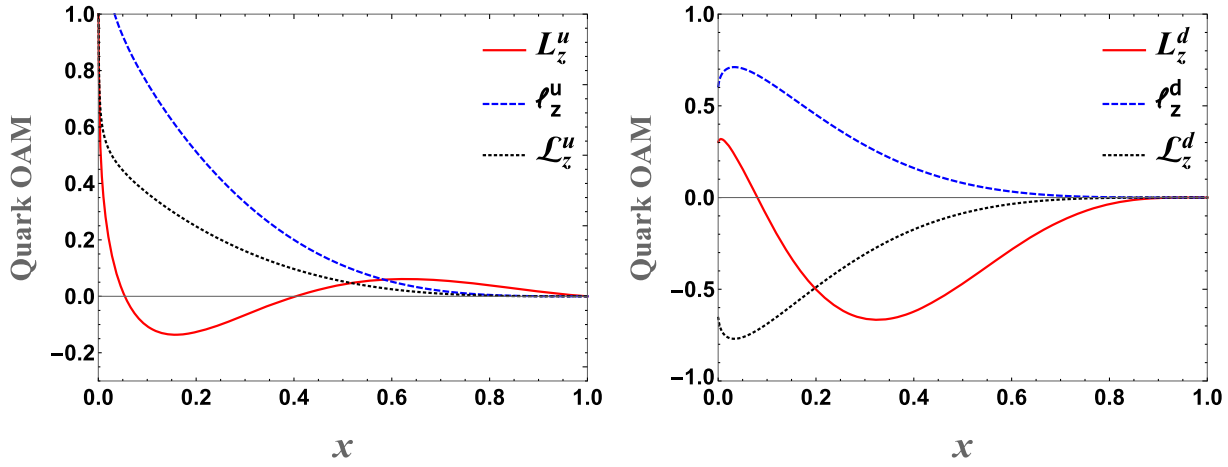

FIG. 6. The variation of canonical OAM $\ell_z^\nu(x)$ and kinetic OAM $L_z^\nu(x)$, as well as $\mathcal{L}_z^\nu$ with longitudinal momentum fraction x, for the u quark and d quarks.

while the kinetic OAM (86) can be calculated from Eqs. (87)–(89). In this model we get $L_z^\nu < 0$ for both the up and the down quarks. The canonical OAM, $\ell_z^\nu > 0$ at $\mu_0 = 0.313$ GeV. This means that the quark OAM is parallel to the proton spin for both u and d quarks. Note also that in a scalar diquark model [51] with AdS/QCD wave functions, the OAM is found to be positive for both quarks. This result is model dependent and may be due to the particular form of the AdS/QCD wave functions. The variations of the canonical quark OAM $\ell_z^\nu(x)$ and the kinetic quark OAM $L_z^\nu(x)$ (given in Eq. (86)) with longitudinal momentum fraction x are shown in Fig. 6 for both u and d quarks. A few interesting points about the OAM in spectator type models are to be noted. In a model without gluons, kinetic and canonical OAM are expected to be equal [5], as the difference between these two are expressed in terms of a gauge potential. The quark OAM was investigated in a simple spectator model with scalar and axial-vector diquarks in [52]. It was found that the relation between the kinetic OAM and the gravitational form factors is not valid in such models, which implied that the kinetic OAM of the quarks is not given by Eq. (86) in such models. In fact, we observed that the kinetic and canonical OAM are not equal in our model, which means that a similar conclusion may be drawn here as well.

In some models, the pretzelosity $h_{1T}^{\perp q}(x, p_T^2)$ (39) distribution is also related to the quark OAM [53–55],

$$\mathcal{L}_z^q = -\int dx d^2\mathbf{p}_T \frac{\mathbf{p}_T^2}{2M^2} h_{1T}^{\perp q}(x, \mathbf{p}_T^2), \tag{98}$$

which in the LFQDQ model has the form

$$\mathcal{L}_z^\nu(x) = \left(C_S^2 N_S^2 - \frac{1}{3} C_A^2 N_0^{\nu 2}\right) \frac{\kappa^2}{M^2 \log(1/x)} \times x^{2a_2^\nu - 2}(1-x)^{2b_2^\nu + 4}. \tag{99}$$

The variation of the $\mathcal{L}_z^\nu$ with x is shown in Fig. 6 for both u and d quarks and is compared with the OAM through GTMDs [Eq. (95)]. In the LFQDQ model we got $\mathcal{L}_z^u > 0$ for the up quark and $\mathcal{L}_z^d < 0$ for down quarks II, while for the scalar diquark model the OAM is $\mathcal{L}_z^\nu > 0$ for both the up and down quarks, as also found in Ref. [23]. The pretzelosity distribution was found not to be related to the quark OAM in a diquark model with axial-vector diquarks [52]; in our model also, as seen in Fig. 6, we find that is it different from the canonical OAM. In [55], it was shown that the pretzelocity TMD in spherically symmetric quark models can be related to the total OAM, however it does not give access to the intrinsic OAM of each quark flavor.

Wigner distributions also allow us to study the correlation between the spin and OAM of the quark, which is given by the operator [5] as

$$C_z^\nu(b^-, \mathbf{b}_T, p^+, \mathbf{p}_T) = \frac{1}{4}\int \frac{dz^- d^2\mathbf{z}_T}{(2\pi)^3} e^{-ip\cdot z} \bar{\psi}^\nu(b^-, \mathbf{b}_T) \times \gamma^+\gamma^5(\mathbf{b}_T \times (-i\partial_T))\psi^\nu(b^- - z^-, \mathbf{b}_T). \tag{100}$$

It can be expressed either in terms of the Wigner distributions ρ_{UL}^ν, or equivalently in terms of the GTMD as

TABLE II. In the light-front AdS/QCD axial-vector diquark model, the values of the canonical OAM ℓ_z^ν; $\mathcal{L}_z^\nu$, and the kinetic OAM L_z^ν for the u, d quarks.

q	u	d
ℓ_z^q Eq. (95)	0.256	0.201
L_z^q Eq. (86)	−0.410	−0.592
$\mathcal{L}_z^q$ Eq. (98)	0.124	−0.218

$$C_z^\nu = \int dx d^2\mathbf{p}_T d^2\mathbf{b}_T (\mathbf{b}_T \times \mathbf{p}_T)_z \rho^\nu_{\mathrm{UL}}(\mathbf{b}_T, \mathbf{p}_T, x)$$
$$= \int dx d^2\mathbf{p}_T \frac{\mathbf{p}_T^2}{M^2} G^\nu_{1,1}(x, 0, \mathbf{p}_T^2, 0, 0). \quad (101)$$

The GTMD $G^\nu_{1,1}(x, 0, \mathbf{p}_T^2, 0, 0)$ in the LFQDQ model has the form

$$G^\nu_{1,1}(x, 0, \mathbf{p}_T^2, 0, 0) = -\left(C_S^2 N_S^2 + C_V^2\left(\frac{1}{3}N_0^2 + \frac{2}{3}N_1^2\right)\right)^\nu \times \frac{1}{16\pi^3}\frac{(1-x)}{x^2}|A_2^\nu(x)|^2 \exp[-a(x)\mathbf{p}_T^2]. \quad (102)$$

For $C_z^\nu > 0$ the quark spin and the quark OAM are aligned, while for $C_z^\nu < 0$ they are antialigned to each other. From Eq. (102), we calculate C_z^ν at $\mu_0 = 0.313$ GeV. In the LFQDQ model the numerical values are $C_z^u = -0.284$ and $C_z^d = -0.234$ for u and d quarks, respectively. $C_z^\nu < 0$ implies that the quark OAM is antiparallel to the quark spin, as observed in the scalar diquark model [51], whereas in the light-cone constituent quark model [5], the C_z^ν values are found to be positive for both u and d quarks. The numerical values of the kinetic OAM [Eq. (86)], and the canonical quark OAM [Eqs. (98) and (95)] for the up and down quarks in the LFQDQ model are given in Table II. The spin contribution of the quark to the proton spin is defined as

$$s_z^\nu = \frac{1}{2}g_A^\nu = \frac{1}{2}\int dx \tilde{H}^\nu(x, 0, 0)$$
$$= \frac{1}{2}\int dx d^2 p_T G^\nu_{1,4}(x, 0, \mathbf{p}_T^2, 0, 0), \quad (103)$$

where g_A^ν is the axial charge, and the GTMD is

$$G^\nu_{1,4}(x, 0, \mathbf{p}_T^2, 0, 0) = \left(C_S^2 N_S^2 + C_V^2\left(\frac{1}{3}N_0^{\nu 2} - \frac{2}{3}N_1^{\nu 2}\right)\right) \times \frac{1}{16\pi^3}\left[|A_1^\nu(x)|^2 - \frac{\mathbf{p}_T^2}{M^2x^2}|A_2^\nu(x)|^2\right] \times \exp[-a(x)\mathbf{p}_T^2]. \quad (104)$$

We should note that the axial charges are highly scale dependent and are measured at high energies, whereas the LFQDQ model has a low initial scale of $\mu_0 = 0.313$ GeV. So we need to consider the scale evolution of the distributions before comparing them with the measured data. For the d quark, the axial charge is known to be negative at larger scales. In Ref. [19] the scale evolution of axial charges are given, where it is shown that the axial charges for the d quarks become negative for $\mu^2 \geq 0.15$ GeV^2. In the LFQDQ model we got the axial charges for the up quark and the down quark as $s_z^u = 1.142$ and $s_z^d = 0.340$ at $\mu_0 = 0.313$ GeV. while at $\mu^2 = 1$ GeV^2 the axial charges for the up quark and the down quarks are given by $s_z^u = 0.73$ and $s_z^d = -0.54$, respectively [19].

A few observations about other calculations in the literature based on diquark models: in [13], a more phenomenological version of a diquark model was used, with the inclusion of both scalar and axial-vector diquarks. The LFWFs were parametrized using fit of polarized and unpolarized pdf data at the lowest scale. It was found that the momentum sum rule cannot be satisfied in such models. The spin sum rule has not been investigated in this reference. The quark OAM has also been investigated in [23] using a LFWF obtained from soft-wall ADs/QCD; the spin sum rule has not been explored in this model. In our model, which follows a similar approach, the parameters in the LFWFs, that consist of one quark and one diquark, are obtained from fits to electromagnetic form factors and pdf data at the initial scale. The spin sum rule constrains the total angular momentum of the diquark.

VII. CONCLUSIONS

As GPDs and TMDs encode information about the three-dimensional structure of the nucleons and their spin and orbital angular momentum, these distributions are being investigated in different models. Both GPDs and TMDs are not physical observables, but many quantities like orbital angular momentum, average momentum of a parton, etc. can be related to different TMDs and GPDs. Though there is no one-to-one correspondence between TMDs and GPDs, they satisfy many interesting relations. Except a few, most of the relations are model dependent. In this work we have explored the possible relations in a light-front quark-diquark model of the proton. An analytic formula for the lensing function has been formulated in this model. The lensing function is model dependent but is independent of quark flavor and is the same for unpolarized quarks in a transversely polarized proton or transversely polarized quarks in an unpolarized proton. Different types of relations with GPDs and TMDs and their momenta are discussed in this model. These relations are important for model building of the distribution functions for the nucleons. We also calculated the quark orbital angular momentum using different relations. The results are compared with other calculations in similar models. It is observed that the kinetic OAM in this model is not the same as the canonical OAM, which is an indication that the total angular momentum of the quark is not expressed in terms of the gravitational form factors, as was also observed earlier in the literature in a diquark spectator model. The pretzelosity distribution in this model also does not give the quark OAM.

ACKNOWLEDGEMENTS

This work is financially supported by Science and Engineering Research Board under the Grant No. CRG/2019/000895.

[1] J. Collins, *Foundations of Perturbative QCD* (Cambridge University Press, Cambridge, England, 2013), Vol. 32.

[2] D. Boer, P. J. Mulders, and F. Pijlman, Universality of T odd effects in single spin and azimuthal asymmetries, Nucl. Phys. **B667**, 201 (2003).

[3] M. Diehl, Generalized parton distributions, Phys. Rep. **388**, 41 (2003).

[4] M. Burkardt, Impact parameter space interpretation for generalized parton distributions, Int. J. Mod. Phys. A **18**, 173 (2003).

[5] C. Lorce and B. Pasquini, Quark wigner distributions and orbital angular momentum, Phys. Rev. D **84**, 014015 (2011).

[6] S. Meissner, A. Metz, and M. Schlegel, Generalized parton correlation functions for a spin-1/2 hadron, J. High Energy Phys. 08 (2009) 056.

[7] M. Burkardt, Chromodynamic lensing and transverse single spin asymmetries, Nucl. Phys. **A735**, 185 (2004).

[8] M. Burkardt, Quark correlations and single spin asymmetries, Phys. Rev. D **69**, 057501 (2004).

[9] S. Meissner, A. Metz, and K. Goeke, Relations between generalized and transverse momentum dependent parton distributions, Phys. Rev. D **76**, 034002 (2007).

[10] B. Pasquini, S. Rodini, and A. Bacchetta, Revisiting model relations between T-odd transverse-momentum dependent parton distributions and generalized parton distributions, Phys. Rev. D **100**, 054039 (2019).

[11] T. Maji and D. Chakrabarti, Light front quark-diquark model for the nucleons, Phys. Rev. D **94**, 094020 (2016).

[12] T. Gutsche, V. E. Lyubovitskij, I. Schmidt, and A. Vega, Light-front quark model consistent with drell-yan-west duality and quark counting rules, Phys. Rev. D **89**, 054033 (2014).

[13] A. Bacchetta, F. Conti, and M. Radici, Transverse-momentum distributions in a diquark spectator model, Phys. Rev. D **78**, 074010 (2008).

[14] S. J. Brodsky, D. S. Hwang, and I. Schmidt, Final-state interactions and single-spin asymmetries in semi-inclusive deep inelastic scattering, Phys. Lett. B **530**, 99 (2002).

[15] D. S. Hwang, Light-cone wavefunction representations of sivers and boer-mulders distribution functions, J. Korean Phys. Soc. **62**, 581 (2013).

[16] T. Maji, D. Chakrabarti, and A. Mukherjee, Sivers and $\cos 2\phi$ asymmetries in semi-inclusive deep inelastic scattering in light-front holographic model, Phys. Rev. D **97**, 014016 (2018).

[17] S. J. Brodsky and G. F. de Teramond, Light-front dynamics and AdS/QCD correspondence: The pion form factor in the space- and time-like regions, Phys. Rev. D **77**, 056007 (2008).

[18] D. Chakrabarti and C. Mondal, Generalized parton distributions for the proton in AdS/QCD, Phys. Rev. D **88**, 073006 (2013).

[19] D. Chakrabarti, T. Maji, C. Mondal, and A. Mukherjee, Quark Wigner distributions and spin-spin correlations, Phys. Rev. D **95**, 074028 (2017).

[20] T. Maji, C. Mondal, and D. Chakrabarti, Leading twist generalized parton distributions and spin densities in a proton, Phys. Rev. D **96**, 013006 (2017).

[21] T. Maji and D. Chakrabarti, Transverse structure of a proton in a light-front quark-diquark model, Phys. Rev. D **95**, 074009 (2017).

[22] T. Maji, D. Chakrabarti, and O. V. Teryaev, Model predictions for azimuthal spin asymmetries for HERMES and COMPASS kinematics, Phys. Rev. D **96**, 114023 (2017).

[23] T. Gutsche, V. E. Lyubovitskij, and I. Schmidt, Nucleon parton distributions in a light-front quark model, Eur. Phys. J. C **77**, 86 (2017).

[24] V. E. Lyubovitskij and I. Schmidt, Scaling of PDFs, TMDs, and GPDs in soft-wall AdS/QCD, Phys. Rev. D **102**, 034011 (2020).

[25] V. E. Lyubovitskij and I. Schmidt, Gluon parton densities in soft-wall AdS/QCD, Phys. Rev. D **103**, 094017 (2021).

[26] V. E. Lyubovitskij and I. Schmidt, New findings in gluon TMD physics, Phys. Rev. D **104**, 014001 (2021).

[27] M. Burkardt, Impact parameter dependent parton distributions and off-forward parton distributions for $\zeta - -- > 0$, Phys. Rev. D **62**, 071503 (2000).

[28] M. Burkardt, Impact parameter dependent parton distributions and transverse single spin asymmetries, Phys. Rev. D **66**, 114005 (2002).

[29] M. Diehl and P. Hägler, Spin densities in the transverse plane and generalized transversity distributions, Eur. Phys. J. C **44**, 87 (2005).

[30] M. Burkardt, Transverse deformation of parton distributions and transversity decomposition of angular momentum, Phys. Rev. D **72**, 094020 (2005).

[31] P. J. Mulders and R. D. Tangerman, The complete tree-level result up to order 1/q for polarized deep-inelastic leptoproduction, Nucl. Phys. **B461**, 197 (1996).

[32] A. Bacchetta, M. Diehl, K. Goeke, A. Metz, P. J. Mulders, and M. Schlegel, Semi-inclusive deep inelastic scattering at small transverse momentum, J. High Energy Phys. 02 (2007) 093.

[33] J. C. Collins, Leading twist single transverse-spin asymmetries: Drell-Yan and deep inelastic scattering, Phys. Lett. B **536**, 43 (2002).

[34] V. Barone, A. Drago, and P. G. Ratcliffe, Transverse polarisation of quarks in hadrons, Phys. Rep. **359**, 1 (2002).

[35] M. Anselmino, M. Boglione, J. Hansson, and F. Murgia, Polarized inclusive leptoproduction, $ln \to hx$, and the hadron helicity density matrix ρ (h): Possible measurements and predictions, Phys. Rev. D **54**, 828 (1996).

[36] C. J. Bomhof, P. J. Mulders, and F. Pijlman, Gauge link structure in quark–quark correlators in hard processes, Phys. Lett. B **596**, 277 (2004).

[37] C. J. Bomhof and P. J. Mulders, Gluonic pole cross sections and single spin asymmetries in hadron-hadron scattering, J. High Energy Phys. 02 (2007) 029.

[38] M. G. A. Buffing, A. Mukherjee, and P. J. Mulders, Generalized universality of higher transverse moments of quark TMD correlators, Phys. Rev. D **86**, 074030 (2012).

[39] M. G. A. Buffing, A. Mukherjee, and P. J. Mulders, Generalized universality of definite rank gluon transverse momentum dependent correlators, Phys. Rev. D **88**, 054027 (2013).

[40] S. J. Brodsky, D. S. Hwang, and I. Schmidt, Final-state interactions and single-spin asymmetries in semi-inclusive deep inelastic scattering, Phys. Lett. B **530**, 99 (2002).

[41] D. Chakrabarti, N. Kumar, T. Maji, and A. Mukherjee, Sivers and Boer–Mulders GTMDs in light-front holographic quark–diquark model, Eur. Phys. J. Plus **135**, 496 (2020).
[42] V. Barone, S. Melis, and A. Prokudin, Boer-mulders effect in unpolarized sidis: An analysis of the compass and hermes data on the cos 2ϕ asymmetry, Phys. Rev. D **81**, 114026 (2010).
[43] M. Burkardt, Hadron tomography, AIP Conf. Proc. **915**, 313 (2007).
[44] M. Burkardt, Sivers mechanism for gluons, Phys. Rev. D **69**, 091501 (2004).
[45] M. Burkardt, Quark correlations and single-spin asymmetries, in *Continuous Advances In QCD 2004* (World Scientific, Singapore, 2004), pp. 64–73.
[46] Z. Lu and I. Schmidt, Connection between the sivers function and the anomalous magnetic moment, Phys. Rev. D **75**, 073008 (2007).
[47] T. Maji, C. Mondal, D. Chakrabarti, and O. V. Teryaev, Relating transverse structure of various parton distributions, J. High Energy Phys. 01 (2016) 165.
[48] C. Lorce and B. Pasquini, On the origin of model relations among transverse-momentum dependent parton distributions, Phys. Rev. D **84**, 034039 (2011).
[49] S. E. Kuhn, J.-P. Chen, and E. Leader, Spin structure of the nucleonstatus and recent results, Prog. Part. Nucl. Phys. **63**, 1 (2009).
[50] X. Ji, Gauge-Invariant Decomposition of Nucleon Spin, Phys. Rev. Lett. **78**, 610 (1997).
[51] D. Chakrabarti, T. Maji, C. Mondal, and A. Mukherjee, Wigner distributions and orbital angular momentum of a proton, Eur. Phys. J. C **76**, 409 (2016).
[52] T. Liu and B.-Q. Ma, Quark angular momentum in a spectator model, Phys. Lett. B **741**, 256 (2015).
[53] J. She, J. Zhu, and B.-Q. Ma, $h_{1T}^{\perp}$ and quark orbital angular momentum, Phys. Rev. D **79**, 054008 (2009).
[54] H. Avakian, A. V. Efremov, P. Schweitzer, and F. Yuan, Transverse momentum dependent distribution functions in the bag model, Phys. Rev. D **81**, 074035 (2010).
[55] C. Lorce and B. Pasquini, Pretzelosity TMD and quark orbital angular momentum, Phys. Lett. B **710**, 486 (2012).